Research Square

Preprints are preliminary reports that have not undergone peer review.
They should not be considered conclusive, used to inform clinical practice,
or referenced by the media as validated information.

Undernutrition Enhances Deoxynivalenol-Induced Neurotoxicity in Rats: Associations with Oxidative Stress, Blood–Brain Barrier-Related Changes, and Ferroptosis-Associated Responses

Sakshi Mishra
CSIR- Central Drug Research Institute
Divyansh Sharma
CSIR- Central Drug Research Institute
Gaurav Jha
CSIR- Central Drug Research Institute
Bhawna Tomar
CSIR- Central Drug Research Institute
Sonam Kanchan
CSIR- Central Drug Research Institute
Anuj Kumar
CSIR- Central Drug Research Institute
Radhika Kapoor
CSIR- Central Drug Research Institute
Sristi Agarwal
CSIR- Central Drug Research Institute
Rabi Bhatta
CSIR- Central Drug Research Institute
Shubha Shukla
CSIR- Central Drug Research Institute
Srikanta Kumar Rath
rathsk_2000@yahoo.com
CSIR- Central Drug Research Institute

Research Article

Keywords: Deoxynivalenol, undernourishment, oxidative stress, cell death, cytokines, neurotransmitters

Posted Date: November 20th, 2026

DOI: https://doi.org/10.21203/rs.3.rs-11564613/v1

License: This work is licensed under a Creative Commons Attribution 4.0 International License.
Read Full License

Additional Declarations: No competing interests reported.

Undernutrition Enhances Deoxynivalenol-Induced Neurotoxicity in Rats: Associations with Oxidative Stress, Blood–Brain Barrier-Related Changes, and Ferroptosis-Associated Responses

[1]Sakshi Mishra, [1]Divyansh Sharma, [1,2]Gaurav Jha, [1,2]Bhawna Tomar, [1,2]Sonam Kanchan, [5]Anuj Kumar [1]Radhika Kapoor, [3]Sristi Agarwal, [3]Rabi Bhatta, [4]Shubha Shukla, [1,2]Srikanta Kumar Rath*

[1]Genotoxicity Laboratory, Division of Toxicology and Experimental Medicine, CSIR-Central Drug Research Institute, Lucknow 226031, Uttar Pradesh, India.

[2]Academy of Scientific and Innovative Research (AcSIR), Ghaziabad, 201002, India.

[3]Division of Pharmaceutics and Pharmacokinetics, CSIR-Central Drug Research Institute, Lucknow 226031 Uttar Pradesh, India

[4]Division of Neuroscience and Ageing Biology, CSIR-Central Drug Research Institute, Lucknow 226031 Uttar Pradesh, India

[5]Regulatory Toxicology Laboratory, Division of Toxicology and Experimental Medicine, CSIR-Central Drug Research Institute, Lucknow 226031, Uttar Pradesh, India.

*To whom all correspondence should be addressed
Srikanta Kumar Rath: E-mail: rathsk_2000@yahoo.com

Abstract

Undernutrition remains highly prevalent in many developing countries, where food quality may be compromised and exposure to food-borne contaminants can coincide with nutritional deficiency. The present study investigated whether undernutrition enhances deoxynivalenol (DON)-induced neurotoxicity and examined associated molecular and biochemical responses using an undernourished rat model. Adult male and female rats were subjected to undernutrition and orally exposed to DON (0.5, 1, and 2.5 mg/kg body weight), with or without glutathione (GSH) supplementation. Behavioural assessments revealed impairments in learning, memory, and anxiety-related behaviour in undernourished rats treated with DON. Histopathological analyses demonstrated dose-dependent neuronal degeneration, particularly within the hippocampus. Brain DON concentrations were markedly higher in undernourished rats, accompanied by reduced expression of BBB tight-junction proteins. DON exposure under undernourished conditions also altered brain neurotransmitter levels, increased pro-inflammatory cytokines, and enhanced oxidative stress, as indicated by increased lipid peroxidation and impaired antioxidant defence. Total brain iron levels were elevated, while molecular analyses showed decreased GPX4 and increased ACSL4 together with altered expression of the autophagy-associated proteins Beclin-1 and LC3. These findings are consistent with ferroptosis- and autophagy-associated responses but do not by themselves establish these pathways as causal mechanisms of neuronal death. GSH supplementation partially ameliorated several DON-induced alterations. Collectively, the findings indicate that undernutrition markedly increases susceptibility to DON-induced neurotoxicity and is associated with increased brain DON exposure, BBB-associated changes, oxidative stress, iron dysregulation, and ferroptosis-associated molecular responses. These findings highlight nutritional status as a potentially important susceptibility factor that warrants consideration in future DON food-safety risk assessments.

Keywords: Deoxynivalenol, undernourishment, oxidative stress, cell death, cytokines, neurotransmitters.

Introduction

The neurotoxic effects of chemical contaminants are frequently evaluated without adequate consideration of nutritional status, despite growing evidence that nutrition plays a critical role in modulating toxic responses in both humans and animals (Reis & Spencer, 2024). Undernutrition, a condition stemming from inadequate intake of food or essential nutrients or from impaired absorption and utilisation, can significantly influence how the nervous system responds to toxic exposures. Importantly, undernutrition may increase susceptibility to chemically induced neurological damage and modify the severity of neurotoxic responses (Spencer & Palmer, 2012).

The combined impact of undernutrition and exposure to neurotoxic food contaminants is particularly relevant for low-income populations where chronic food insecurity is a persistent reality (Siddiqui et al., 2020). This includes rural communities, especially in rain-fed regions of low-income countries where environmental variability often disrupts food availability and the urban poor, who may struggle to access sufficient and nutritious food due to economic constraints (Tchonkouang et al., 2024).

Among foodborne contaminants, mycotoxins represent a persistent global concern for food safety and public health. According to estimates by the Food and Agriculture Organization (FAO), approximately 25% of global crop production is affected by various mycotoxins each year, leading to an annual loss of nearly one billion tons of food and food products (Eskola et al., 2019). Chronic dietary exposure to mycotoxins affects billions of people worldwide through commonly consumed foods such as cereals, spices, dairy products, meat, coffee, wine, and beer(Stoev, 2024). According to the World Health Organization (WHO, 2016), an estimated 500 million people in economically challenged regions of the developing world are regularly exposed to naturally occurring toxins, including mycotoxins, through their daily diet.

The risk is especially significant in children, who consume more food relative to their body weight than adults, potentially increasing their vulnerability to mycotoxin exposure (Lombard, 2014).

Among various mycotoxins, Deoxynivalenol (DON) stands out as one of the most frequently detected mycotoxins, particularly in cereal-based products, making it a prevalent environmental contaminant that causes food refusal and growth retardation in both humans and animals (Jia et al., 2023). A recent global survey conducted in 2024 reported a severe ongoing risk to livestock food safety, noting that over 75% of all agricultural samples tested positive for multiple mycotoxins simultaneously. (Firmenich, 2024). High contamination rates have been reported across multiple regions, including East Asia, Europe, the Americas, and Africa (Gruber-Dorninger et al., 2019). In a survey from China, DON was detected in 91.5% of wheat samples, with a median concentration of 154 μg/kg and a maximum level reaching 1.130 mg/kg (Liu et al., 2016). Other regions have also reported significant DON contamination. For instance, in the United States, DON was detected in 94% of swine feed samples and in 88.2% of corn silage samples, with certain cases exceeding 5 mg/kg (Weaver et al., 2021). Additionally, in Brazil, DON was detected in 77.9% of wheat flour samples, with the highest concentration reported at 2.794 mg/kg (Silva et al., 2018). A recent study from Italy investigated the presence of regulated mycotoxins in 3769 maize grain samples collected from 88 storage centres by the National Monitoring Network over 11 years (2011–2021). Maize lots from a drying and storage centre in 2014 reported extremely high levels reaching 36 mg/kg, where 100% of the analysed samples tested positive for DON (Locatelli et al., 2022).

While acute exposure to high DON doses leads to overt toxicity, chronic exposure to low concentrations is associated with cytotoxic, immunotoxic, neurotoxic, and reproductive effects (Claeys et al., 2020; Deng et al., 2023; Pestka, 2010). Understanding the ecological safety of DON contamination requires a comprehensive grasp of its toxicological mechanisms. DON

146 exerts harmful effects on both humans and animals. Studies indicate that global warming may
147 increase the prevalence of mycotoxins in crops. Since DON is not entirely degraded during
148 food processing and is stable during extreme cooking conditions, therefore its presence in food
149 poses a direct risk to human health (Mishra, Dixit, et al., 2014). These factors collectively
150 underscore the growing concern regarding exposure to mycotoxins, particularly DON.

151 DON-induced neurotoxicity has been linked to activation of mitogen-activated protein kinase
152 (MAPK) signalling, mitochondrial dysfunction, oxidative stress, and apoptotic pathways (Cao
153 et al., 2021; Wang et al., 2018). Following its ability to cross the blood brain barrier (BBB),
154 DON directly affects neurons and glial cells, leading to astrocytic and microglial dysfunction
155 and neuroinflammatory responses (Razafimanjato et al., 2011). This disruption leads to an
156 inflammatory response within the central nervous system, which has been associated with
157 alterations in brain dopamine levels and reductions in ganglion areas, contributing to significant
158 neural damage (Wang et al., 2020). With increasing DON concentrations, oxidative damage
159 has also been reported in the cerebral cortex, cerebellum, and hippocampus of piglets (Wang
160 et al., 2020). Our previous studies also suggested that DON disrupts mitochondrial function in
161 neuronal SH-SY5Y cells by inducing oxidative stress and calcium imbalance, leading to
162 increased mitochondrial fission, reduced ATP production, and activation of autophagy
163 pathways (Mishra et al., 2024). Evidence also suggests that DON compromises the integrity of
164 the BBB and exerts cytotoxic effects on human cerebral microvascular endothelial cells
165 (Behrens et al., 2015; Prelusky et al., 1990). This disruption of the BBB may not only facilitate
166 DON's own entry into the brain but could also allow passage of other mycotoxins that would
167 otherwise be excluded.

168 In developing regions, mycotoxin exposure frequently coincides with undernutrition,
169 gastrointestinal dysfunction, and infectious diseases, particularly among young children
170 (Watson et al., 2017). Undernutrition is known to impair antioxidant defences and

mitochondrial function (Bañuls et al., 2019), which may exacerbate DON-induced oxidative stress, neuronal injury, and inflammatory responses. Despite the clear biological plausibility of such interactions, systematic experimental studies investigating the combined effects of undernutrition and DON exposure on neurotoxicity remain scarce.

Therefore, the present study aimed to investigate whether chronic undernutrition exacerbates DON-induced neurotoxicity using a controlled rat model. By integrating phenotypic, biochemical, histological, and molecular endpoints, this work examines how nutritional status modulates neurotoxic outcomes following dietary DON exposure. Particular emphasis was placed on brain DON availability, BBB-associated proteins, oxidative stress, iron homeostasis, and ferroptosis- and autophagy-associated molecular responses. Given the coexistence of undernutrition and dietary mycotoxin exposure in resource-limited settings, the findings may provide a basis for considering nutritional status as a susceptibility factor in future food-safety risk assessment.

Materials and Methods

Chemicals and Reagents

DON and reduced L-Glutathione (GSH) were obtained from Sigma-Aldrich (St. Louis, MO, USA). DON and GSH were prepared in physiological saline (0.9 % NaCl) and administered via oral gavage. Assay kits for total superoxide dismutase (T-SOD; E-BC-K019-S), malondialdehyde (MDA; E-BC-K025-S), glutathione peroxidase (GPX; E-BC-K809-M), and catalase (CAT; E-BC-K031-M) were sourced from Elabscience (Texas, USA). Enzyme-linked immunosorbent assay (ELISA) kits for noradrenaline/norepinephrine (NA/NE; E-EL-0047), dopamine (DA; E-EL-0046), serotonin/5-hydroxytryptamine (5-HT; E-EL-0033), and a colorimetric assay kit for γ-aminobutyric acid (GABA; E-BC-K852-M) were also procured from Elabscience. The iron assay kit (MAK025) was purchased from Merck KGaA (Darmstadt, Germany). Cytokine detection kits for IFN-γ, IL-1β, IL-18, IL-12, IL-6, and IL-

10 were likewise obtained from Elabscience. Fluorojade B (TR-150-FJB) was obtained from Thebarton, Australia. All reagents and chemicals used in the study were of analytical grade and met the highest quality standards available.

Animals and ethics statement

Male and female Wistar rats, aged 5 to 6 weeks and weighing between 180–220 g, were obtained from the breeding colony at CSIR-Central Drug Research Institute (CSIR-CDRI), Lucknow. The animals were acclimated to standard laboratory conditions and provided with a commercial pellet diet and water ad libitum. They were housed in plastic cages with rice husk bedding, maintained under controlled environmental conditions temperature of 22 ± 2°C, relative humidity of 50–60%, and a 12-hour light/dark cycle in accordance with the guidelines set by the Animal Welfare Committee of CSIR-CDRI. All experimental procedures involving animals were reviewed and approved by the Institutional Animal Ethics Committee (IAEC) of CSIR-CDRI (Approval No. IAEC/2022/74/Renew-0/Sl no.47, dated 05/07/2022).

Experimental Design and diet

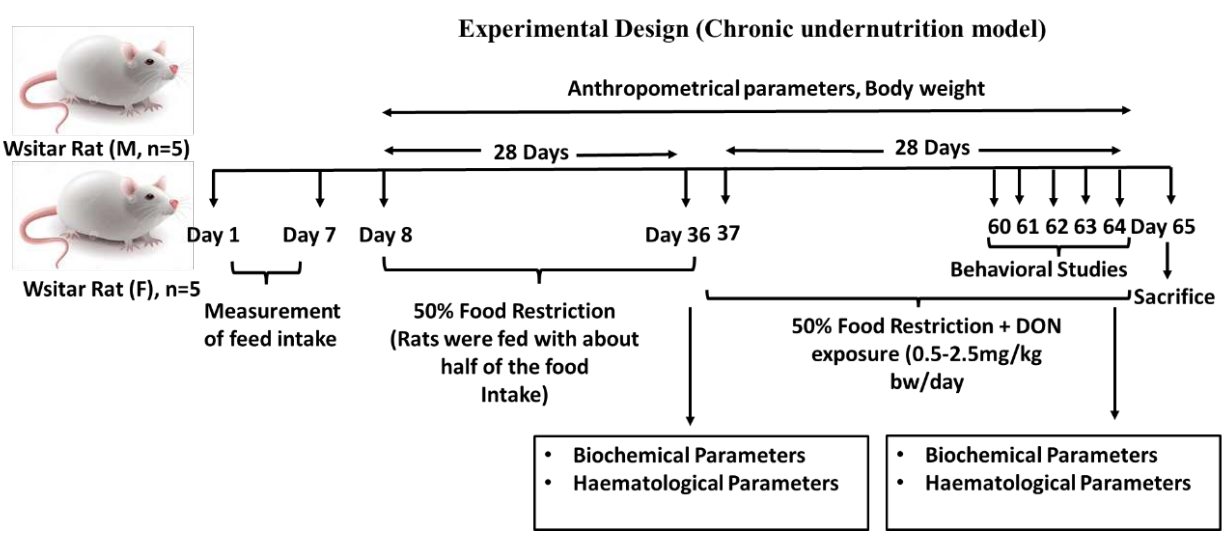

Rats were randomly divided into various groups following the protocol described earlier (Quiróz-González et al., 2013). All animals were provided with unrestricted access to a standard commercial diet and water during a 7-day acclimatization period. Daily food intake was recorded throughout this period. Nine experimental groups (n = 10 per group; 5 males and 5 females) were a priori defined before commencement of any interventions. From Day 1 to Day 7 feed intake was calculated and from day 8, groups designated as undernourished (Group III, Group V–Group IX) received a 50% dietary restriction regimen, while the remaining groups maintained ad libitum feeding, as outlined in previous studies (Cesani et al., 2003; Hardikar et al., 2015; Vázquez-Mendoza et al., 2017). No pharmacological agents neither DON nor GSH were administered during this induction phase. On Day 37, the respective treatments were initiated according to the groups assigned below. The pre-specification of groups ensured consistency in experimental nomenclature across all study phases and avoided retrospective re-labelling; importantly, this approach clarifies that the only variable during Days 7–36 was dietary intake, with pharmacological exposures beginning thereafter, thereby enhancing transparency and methodological rigour in accordance with ARRIVE guidelines.

i. **Group I (Control):** Continued on standard diet without additional treatment.

ii. **Group II (DON alone):** Administered 2.5 mg/kg body weight/day of DON with standard diet.

Simultaneously, the undernourished group was split into six subgroups (n=10; 5 males and 5 females per group) as follows:

iii. **Group III (UN alone):** Continued on restricted diet without additional treatment.

iv. **Group IV (GSH alone):** Administered 49.6 mg/kg body weight/day of glutathione (GSH), calculated from a human equivalent dose (500 mg/day) using a conversion factor of 6.2 for rats (Nair & Jacob, 2016) With standard diet.

v. **Group V (DON 0.5 + UN):** Received 0.5 mg/kg bw/day DON under restricted diet.

vi. **Group VI (DON 1.0 + UN):** Received 1.0 mg/kg bw/day DON under restricted diet.

vii. **Group VII (DON 2.5 + UN):** Received 2.5 mg/kg bw/day DON under restricted diet.

viii. **Group VIII (DON 1.0 + UN + GSH):** Received 49.6 mg/kg bw/day GSH and 1.0 mg/kg bw/day DON under restricted diet.

ix. **Group IX (UN + GSH):** Received 49.6 mg/kg bw/day GSH under restricted diet

Throughout the treatment period, body weight was recorded weekly. Anthropometric, biochemical, and haematological assessments were carried out as described in subsequent sections.

Anthropometrical analysis

To assess nutritional status, all rats were weighed daily using a digital balance throughout the experiment. At the end of the undernourishment phase and DON exposure period (i.e., days 36 and 64, respectively), the weight gain percentage was calculated by dividing the final body weight (on days 36 and 64) by the initial weight (on days 8 and 37) for the respective groups (control and undernourished). Body length (measured from the nose to the anus) was recorded weekly using a flexible measuring tape. In addition, abdominal circumference (measured just anterior to the forelimbs) and thoracic circumference (measured just posterior to the forelimbs) were measured weekly in all animals. These measurements; body weight, body length, and circumferences, were used to compute various anthropometric indices as described below-

- **Body mass index (BMI) = body weight (g)/length2 (cm2)**
- **Lee index= cube root of body weight (g) /nose-to-anus length (cm) (Bernardis & Patterson, 1968)**

Weight-for-Age Relationship (WA)

As described by Anstead et al., a malnutrition scale was employed based on the classification proposed by Gómez et al., Gómez et al. (31), which evaluates the nutritional status of animals

using the weight-for-age (WA) index. This parameter provides a comparative measure of growth retardation relative to a reference standard. The WA index was calculated using the following formula:

Weight for Age (%) = (final weight of undernourished rats/expected weight of undernourished rats based on control rats) × 100

This classification allows for stratification of the degree of undernutrition based on the percentage of expected weight achieved by the experimental animals. Analogous to human clinical classifications, the Anstead model categorises the severity of undernutrition in rodents based on the calculated WA values. According to this model:

Rats with WA values between 76% and 90% are considered to exhibit mild undernutrition.

WA values ranging from 61% to 75% indicate moderate undernutrition.

WA values of 60% or below are classified as severe undernutrition.

This classification system provides a standardised approach to evaluate and compare the nutritional status of animals in experimental settings (Ferreira-Paes et al., 2021).

Haematological analysis

As outlined in the experimental schematic, haematological evaluations were performed at two critical time points: on day 36 (following the establishment of the undernutrition model) and on day 64 (after completion of DON and GSH treatments in undernourished rats, just before sacrifice). For each assessment, approximately 500 µL of blood was collected from individual animals into tubes containing 10 µL of EDTA to prevent clotting. Blood samples were analysed using an automated haematology analyser (Sysmex XT-2000i), which provided a comprehensive profile of haematological parameters. Analyser provided a detailed assessment of various haematological parameters, including WBC, White blood cell count; RBC, red blood

cell count; HGB, haemoglobin; MCV, mean corpuscular volume; MCH, mean corpuscular haemoglobin; MCHC, mean corpuscular haemoglobin concentration; PLT, platelet; NEUT, neutrophils; LYMPH, lymphocytes; MONO, monocytes, EO, eosinophils; BASO, basophils. These parameters enabled a detailed evaluation of blood composition and provided insights into the physiological effects of undernutrition and mycotoxin exposure.

Serum Biochemical analysis

As described in Section 2.5, blood samples were collected from all animals for biochemical analysis. A volume of 500 µL of blood was drawn from each rat and transferred into anticoagulant-free tubes. The samples were allowed to clot at room temperature for approximately one hour, after which they were centrifuged at 4000 rpm for 10 minutes to separate the serum. The resulting serum was carefully collected into cryovials and stored at –80 °C until further analysis. The Erba mamheim XL-200 was used to measure GPT, Glutamic pyruvic transaminase; GOT, Glutamic oxaloacetate transaminase, ALPU, alkaline phosphatase; CRE, Creatinine, PHOS, Phosphorous, UREA, BUN, Blood urea nitrogen; GLU, Glucose; TG, Total Triglycerides; CHOL, Total cholesterol; CA, Calcium; ALB, Albumin; PRO, Total Protein, BIT1, Total Bilirubin.

Behavioural parameter

To minimise stress-induced variability, behavioural testing was conducted over a span of five consecutive days, with only one behavioural assay performed per day. Following each test, all animals were returned to their home cages and maintained under controlled environmental conditions to allow for recovery and to prevent any residual effects from influencing subsequent behavioural assessments.

Elevated Plus Maze (EPM) test

To assess anxiety-like behavior, the Elevated Plus Maze (EPM) test was conducted on day 60. The apparatus consisted of a plus-shaped maze elevated 61 cm above the floor, comprising two opposing open arms (50 × 10 cm) and two closed arms of the same length and width, but enclosed by 30 cm high walls (50 × 10 × 30 cm). The arms intersected at a central platform measuring 10 × 10 cm. At the beginning of each trial, the rat was placed at the centre of the maze, facing an open arm, and allowed a 2-minute habituation period to explore the environment. Following habituation, the test phase lasted 5 minutes, during which the rat was again placed at the centre, facing an open arm, and permitted to explore the maze freely. The time spent in the open arms was recorded as an index of anxiety, with observations made by two independent researchers who were blinded to the treatment groups. To eliminate olfactory cues, the maze was thoroughly cleaned with 10% ethanol between each trial (Kraeuter et al., 2019). After the behavioural assessments, animals were euthanized. The brains were immediately harvested, rinsed to remove blood, and processed for biochemical, neurochemical, enzymatic, and histological analyses.

Morris Water Maze (MWM) test

MWM test was used to evaluate spatial learning and memory following DON and GSH treatments, based on previously described protocols (Mishra et al., 2018; Tiwari et al., 2021). The test was conducted using a circular pool (132 cm in diameter × 75 cm in height) filled with water maintained at 25 ± 0.5 °C. A hidden platform was submerged just below the water surface and remained in a fixed location throughout the training trials. Behavioural testing was performed on days 61–63 post-treatment to assess learning and memory acquisition, followed by a probe trial on day 64. On each training day, animals were placed in the pool and allowed to locate the hidden platform. Each trial ended either when the rat located the platform or after a maximum duration of 2 minutes. Escape latency (the time taken to find the platform) was recorded during each trial. On day 64, the platform was removed, and a probe trial was

conducted in which each rat was allowed to swim freely for 1 minute. The time spent in the target quadrant (where the platform was previously located) was recorded to evaluate memory retention. Behavioural data were captured and analysed using AnyMaze tracking software.

Histopathology

Tissue block preparation and sectioning

Following euthanasia on day 65, the rat brains were carefully excised and immersion-fixed in 4% paraformaldehyde until further processing. For dehydration, tissue sections were passed sequentially through ascending concentrations of isopropanol and cleared in xylene, following established protocols. The processed sections were then mounted on poly-L-lysine-coated glass slides in preparation for histological staining.

Cresyl Violet (CV) staining

Cresyl violet staining was employed to evaluate potential morphological changes in neuronal structures. Initially, paraffin-embedded brain sections were deparaffinized in xylene and rehydrated through a descending ethanol series (100%, 90%, 70%), followed by a brief rinse in distilled water. Sections were then incubated in 0.5% cresyl violet solution at 37°C for 30 minutes. After staining, slides were rinsed with distilled water, and differentiation was achieved by progressive dehydration through ethanol (70%, 90%, 100%), finishing with a final xylene wash. The slides were mounted using DPX mounting medium and examined under a Nikon light microscope at 40× magnification to visualise neuronal architecture.

Fluoro-Jade B (F-J B) histo-fluorescence staining

Fluoro-Jade B (F-J B), a a marker of neuronal degeneration, , was employed to assess neuronal degeneration or cell death in the brain following DON exposure. The histofluorescence staining was carried out following a modified version of established protocols. First, brain sections were

incubated in 0.06% (w/v) potassium permanganate (prepared in distilled water) at room temperature for 20 minutes. After this, they were stained with 0.0004% F-J B (Biosensis, Thebarton, Australia) dissolved in 0.1% glacial acetic acid, again at room temperature, for 40 minutes. Finally, the sections were dehydrated and mounted under coverslips using dibutylphthalate polystyrene xylene (DPX; Sigma, St. Louis, MO, USA) as the mounting medium. Fluoro-Jade B labelled degenerating neurons are visualised with blue light excitation (like those used for visualising fluorescein or FITC) under a Nikon fluorescence microscope at 40× magnification

Neurochemical analysis

To quantify levels of major biogenic amines, frozen brain tissues were homogenised in accordance with the protocols provided by the kit manufacturer. Concentrations of noradrenaline/norepinephrine (NE); (E-EL-0047), dopamine (DA); (E-EL-0046), serotonin/5-hydroxytryptamine (5-HT); (E-EL-0033), and γ-aminobutyric acid (GABA); (E-BC-K852-M) were determined using commercially available ELISA and colorimetric assay kits from Elabscience (Texas, USA) respectively.

Measurement of antioxidant enzymes

Whole brain homogenates (10% w/v) were prepared to evaluate oxidative stress markers, and enzymatic assays. Commercial kits (Elabscience, Texas, USA) were used to measure the activity of total superoxide dismutase (T-SOD; E-BC-K019-S), glutathione peroxidase (GPX; E-BC-K809-M), catalase (CAT; E-BC-K031-M), and the lipid peroxidation marker malondialdehyde (MDA; E-BC-K025-S), as per the manufacturers' guidelines.

Assessment of tissue cytokine concentrations

Cytokine levels in brain homogenates were quantified to assess the neuroinflammatory response. Commercial rat-specific Enzyme-Linked Immunosorbent Assay (ELISA) Kits from

Elabscience, Texas, USA were employed to measure the concentrations of interferon-gamma (IFN-γ), interleukin-1 beta (IL-1β), IL-6, IL-10, IL-12, and IL-18, following the manufacturer's instructions.

Measurement of iron accumulation

Total iron accumulation in brain tissues was determined using a colorimetric iron quantification kit (MAK025, Merck KGaA, Darmstadt, Germany). Tissue lysates were processed according to the manufacturer's protocol.

Western blotting

Proteins were extracted from brain tissue by lysing the tissue in RIPA buffer (Himedia, TCL131, India) supplemented with protease and phosphatase inhibitors to prevent degradation and dephosphorylation. After centrifugation, total protein concentrations were measured using the Bradford assay (Himedia, ML106, India). Equal amounts of protein were separated by SDS-PAGE, and the resolved proteins were transferred onto a PVDF membrane (GE Amersham, #1060023, UK). The membrane was blocked at room temperature for 1 h in TBST (20 mM Tris–HCl, 150 mM NaCl, 0.1% Tween-20) containing 5% BSA, followed by an overnight incubation at 4 °C with primary antibodies: Occludin (Cell Signaling Technology, E684R, USA), ZO-1 (Proteintech, catalog 21773-1-1AP, rabbit polyclonal), Claudin-5 (Proteintech, 29767-1-AP, rabbit polyclonal), GPX4 (Proteintech, 67763-I-IG, mouse monoclonal), ACSL4 (Proteintech, 22401-1-AP, rabbit polyclonal), BDNF (Cell Signaling Technology, 47808S, rabbit), Beclin-1 (Cell Signaling Technology, 3495T, rabbit), and LC3 (Cell Signaling Technology, 12741T, rabbit).

After washing the membrane in TBST, HRP-conjugated secondary antibodies (goat anti-rabbit IgG, CST #7074S, USA; goat anti-mouse IgG, CST #7076P2, USA) were applied at a 1:10,000 dilution. Protein bands were visualized using an enhanced chemiluminescence substrate (Bio-

Rad ECL Kit, #175,061, India), and the intensity of each band was quantified by densitometry using ImageJ software.

Determination of DON concentrations in brain tissue following oral administration

LC-MS/MS conditions

The quantification of DON was performed using a Shimadzu Nexera XS Series Liquid Chromatographic and Mass Spectrometric System (LCMS-8050, Kyoto, Japan). The chromatographic separation was performed using a Waters Symmetry C18 analytical column (150 mm × 4.6 mm, 5 µ) and an isocratic mobile phase composed of 85% acetonitrile and 15% deionized water containing 0.2% acetic acid. The LC parameters, such as the temperature of the column oven, the volume of injection, the duration of the run, the temperature of the autosampler, and the flow rate, were maintained at 40°C, 20 µL, 5 minutes, 15°C, and 0.6 mL/min, respectively. The MS parameters for DON have been carefully tuned to get a molecular mass of 296.319 Da with exceptional precision. The necessary optimisations were conducted to determine the stable precursors (Q1) and product ions (Q3). Argon serves as the collision gas in the ongoing production of Q3. Rosuvastatin (RSV) was used as the internal standard (IS) in this investigation. The software provided by Shimadzu Lab Solutions was used comprehensively for every aspect of the procedure, encompassing operation, measurement, and analysis. Table 1 presents a tabulated display of the compound's properties that are based on mass spectrometry.

Time-course assessment of DON concentrations in brain tissue

Following completion of the treatment period, the final DON dose was administered orally, and brain tissue was collected at predetermined post-dose intervals (15, 30 and 60 min) to assess the time-dependent concentrations of DON in brain tissue. Animals were anaesthetised before brain collection, and the excised tissue was stored at −80 °C until analysis by LC–

MS/MS. The tert-butyl methyl ether (TBME) was used as the solvent in the liquid-liquid extraction (LLE) technique to extract both the analyte and the internal standard (IS). In summary, 100 µL of homogenized brain sample, 3mL of organic solvent (TBME) containing 50ng of IS. The mixture was vigorously agitated using a vortex mixer for a duration of 5 minutes and thereafter subjected to centrifugation at a force of 5000 g for 20 minutes. The 2.5 mL of supernatant was collected and dried under nitrogen gas. After the drying process, the samples were reconstituted using 100 µL of acetonitrile and then analyzed using LC-MS/MS. The measurement and analysis of biological samples were performed using LabSolutions software.

Statistical analysis

GraphPad Prism 5 (GraphPad Software, San Diego, California, USA) was used for all statistical analyses. Data are presented as mean ± SD unless otherwise indicated in the figure legends. One-way or two-way analysis of variance (ANOVA), followed by the indicated multiple-comparison procedures, was used for experiments involving more than two groups. Statistical significance was defined as $p < 0.05$. For analyses involving both male and female animals, sex was considered as a biological variable and sex-by-treatment interactions were evaluated where applicable; behavioural analyses were pooled only where no significant interaction was detected. The specific statistical test and comparison groups are indicated in the corresponding figure legends.

Results

Rat Model of Undernutrition

Dietary restriction impairs growth and reduces body mass

All animals were weighed daily throughout the 28-day dietary manipulation period. At the initiation of dietary restriction (Day 8), mean body weights across groups ranged from 180 to 220 g. Rats subjected to a 50% restricted diet (Groups III and V–IX) showed a significant

reduction in body weight beginning on Day 2 after diet restriction ($p \leq 0.005$), whereas rats with ad libitum access to food (Groups I, II, and IV) maintained normal weight gain. Weight loss in the restricted groups persisted until Day 36, with reduced body mass evident at the time of DON/GSH administration. Sex-stratified analysis revealed that undernourished male rats lost approximately 13–19% of body weight, while undernourished females lost 13–18%, with both reductions being significant compared with nourished controls ($p \leq 0.005$) (Fig. 1A and C).

To further assess nutritional status using phenotypic indicators such as thoracic, abdominal circumference and body length were measured weekly following the initiation of dietary restriction (Table S1). Rats maintained on the restricted diet exhibited delayed linear growth compared with nourished controls, with statistically significant differences observed by day 6 after diet reduction. Nourished rats (Groups I, II, and IV) demonstrated a progressive increase in body length and AC/TC ratio over the 28-day experimental period, whereas animals of Groups III and V–IX, receiving a 50% restricted diet, showed a markedly slower rate of length gain and AC/TC ratio (Table S1). Body mass index (BMI), calculated using body weight and body length, was significantly reduced in undernourished rats compared with nourished animals (Fig. 1B and D).

Undernutrition alters haematological and biochemical parameters

On day 36 following the initiation of dietary restriction, rats were anaesthetised for haematological and biochemical assessments. Blood samples were collected, and serum was separated by centrifugation for biochemical analyses. Undernourished rats exhibited significant alterations in haematological parameters, including reduced total white blood cell (WBC) and lymphocyte counts compared with nourished rats across the group I, II and IV, suggesting a suppressive effect of undernutrition on immune status. Mean corpuscular volume (MCV), mean corpuscular hemoglobin (MCH), and mean corpuscular hemoglobin concentration

(MCHC), were significantly higher in nourished rats than in undernourished male and female rats (Table S2).

Biochemical parameters commonly used as indicators of nutritional status were also markedly affected by dietary restriction. Serum glucose levels were significantly lower in undernourished rats relative to nourished animals. Markers of protein and nitrogen metabolism, including albumin, total protein, creatinine, and urea, were significantly reduced in both male and female undernourished rats, whereas serum cholesterol levels were notably depleted (Table S3). Collectively, these alterations highlight the systemic biochemical disturbances associated with chronic undernutrition.

Dietary restriction induces moderate undernutrition

Weight-for-age (WA) was calculated for all experimental groups throughout the study period. One day after the initiation of dietary restriction, WA values in nourished male rats (Groups I, II, and IV) were 100%, 94.9%, and 94.4%, respectively; however, corresponding values in nourished female rats were 100%, 87.6%, and 88.2%. By the end of the experiment (day 36), undernourished male rats (Groups III and V–IX) exhibited WA values of 64.32%, 67.85%, 66.22%, 67.52%, 63.77%, and 68.97%, respectively (Table 2). Similarly, WA values in undernourished female rats from Groups III and V–IX were 66.31%, 65.94%, 65.20%, 69.36%, 63.91%, and 60.61%. The marked reduction in WA values confirms that the restricted feeding regimen successfully induced a state of moderate undernutrition in both male and female rats.

DON exposure to undernourished rats

DON exposure alters anthropometric deficits, impairs growth and reduces BMI in undernourished rats

Anthropometric assessment demonstrated that undernourished rats exposed to DON exhibited significantly reduced body weight, accompanied by a marked decrease in body mass index (BMI) and an approximately 20% reduction in body length compared with controls (Table S4

; Fig. 1E & F). In contrast, rats in the control, and GSH groups showed normal increases in body length and body weight over the study period. While DON exposure alone resulted in a significant reduction in body weight and BMI in both male and female rats relative to controls, body weight and length remained significantly higher than those observed in DON groups. Notably, DON treatment in undernourished rats did not significantly alter body length when compared with undernourished only animals of either sex, however, BMI was partially but significantly decreased in female rats. Pretreatment with GSH led to a partial but significant improvement in BMI in DON-exposed undernourished rats, without producing a significant change in body length.

DON alters haematological and biochemical parameters in undernourished rats

Haematological analysis revealed a further dose-dependent reduction in WBC/total leukocyte counts in DON-exposed undernourished rats both male and female compared with undernourished only groups (Table S5). Pretreatment with GSH significantly increased leukocyte counts, restoring them toward levels observed in control and DON-alone groups.

Biochemical evaluation demonstrated that DON treatment in undernourished rats significantly reduced serum levels of GPT, GOT, and ALP. In contrast, co-administration of GSH with DON in undernourished rats significantly ameliorated these alterations, partially restoring biochemical parameters toward control values (Table S6). These findings collectively indicate that DON exposure in the context of undernutrition is associated with growth deficits and alterations in haematological and biochemical parameters.

Effect of DON on anxiety-like behaviour in undernourished rats (elevated plus maze)

It was observed that DON treated undernourished rats (1-2.5mg/kg) demonstrated pronounced anxiety-like behaviour, characterised by a significant reduction in time spent in the open arms of the maze compared with all control, undernourished and nourished DON alone groups (Fig. 2A). In contrast, GSH administration partially reversed DON-induced anxiety-like behaviour

in undernourished rats, as indicated by increased open-arm exploration as compared to nourished DON alone group (2.5mg/kg). These findings suggest that undernourishment potentiates DON-induced neurobehavioral alterations, while antioxidant supplementation confers measurable behavioural protection. Sex was initially included as a biological variable in behavioural analyses. As no significant sex vs treatment interactions were observed for Morris water maze or elevated plus maze parameters, data from male and female rats were combined for final analysis (n = 10 per group) to enhance statistical robustness.

Effect of DON on spatial learning and memory in undernourished rats (Morris water maze)

Undernourished rats exposed to DON (1 and 2.5 mg/kg) exhibited significant deficits in spatial learning and memory as compared to undernourished or nourished DON alone group (2.5mg/kg). This was evidenced by a longer escape latency and path length across the three consecutive training days in the Morris water maze. Additionally, DON-treated undernourished rats showed a significant reduction in the percentage of time spent in the target quadrant during the probe trial compared with both control and DON-alone (2.5mg/kg) groups (Fig. 2B–D). Pretreatment with GSH significantly attenuated DON-induced impairments under undernourished conditions, as reflected by reduced escape latency and path length and increased target quadrant occupancy relative to the DON+UN group (1mg/kg). Collectively, these results indicate that DON impaired spatial learning and memory in undernourished rats at 1–2.5 mg/kg, while GSH pretreatment partially ameliorated these behavioural alterations.

Effect of DON on neuronal integrity and degeneration in the brain of undernourished rats

Histopathological evaluation revealed marked alterations in neuronal integrity following oral exposure to DON in undernourished rats, particularly within the hippocampus and cortical regions. Cresyl violet staining demonstrated a dose-dependent loss of neurons in the

hippocampus, characterised by neuronal degeneration and a significant reduction in neuronal density in DON-treated groups. Neuronal damage was significantly more pronounced in undernourished rats exposed to DON (2.5mg/kg) compared with animals receiving DON alone (2.5mg/kg) or undernourishment alone, whereas no significant histological changes were observed at the lowest dose (0.5 mg/kg). Notably, female undernourished rats exhibited significantly greater neuronal loss following DON exposure at 1 mg/kg and 2.5 mg/kg compared with male rats treated with the same dose regime.

Consistent with these findings, Fluoro-Jade staining of cortical sections revealed minimal neuronal degeneration in control animals, as indicated by the presence of only a few stained cells (Fig. 4). A significantly modest increase in Fluoro-Jade positive cells was observed in rats treated with DON alone, while undernourishment alone resulted in levels comparable to control animals. In contrast, undernourished rats exposed to DON at doses of 1 mg/kg and 2.5 mg/kg showed a significant increase in the number of Fluoro-Jade positive cells in the cortex, indicating enhanced neuronal degeneration.

Time-dependent brain concentrations of DON under undernourished conditions

Brain DON concentrations were assessed at defined intervals following the final oral dose. The highest measured concentration in undernourished DON-treated rats (2.5mg/kg) was 218.14 ng/mL at 30 min, followed by a decline at 60 min. The time-dependent brain DON concentration profile and associated pharmacokinetic measurements are presented in Fig. 5A. In contrast, well-nourished rats receiving DON (2.5mg/kg) exhibited substantially lower measured brain DON concentrations, with a peak level of 27.05 ng/mL occurring at 30 min post-administration. These findings indicate differences in measured brain DON concentrations between the experimental groups under the conditions studied. As the present experiment measured DON in brain tissue rather than plasma, the data do not by themselves distinguish altered gastrointestinal absorption or systemic disposition from altered transfer

across the BBB. Co-administration of glutathione (GSH) did not significantly alter DON availability to the brain. Brain tissue DON concentrations in GSH-treated undernourished rats were comparable to those observed in the DON treated (1 mg/kg) undernourished group, indicating that GSH did not markedly influence DON distribution with respect to BBB passage. No significant differences in total brain weight were observed among control, undernourished, or lower-dose DON-treated groups. However, a moderately significant reduction in brain weight was detected in undernourished rats exposed to the highest dose of DON (2.5 mg/kg) compared with control animals. Importantly, this reduction was comparable in both male and female rats, with no significant sex-dependent differences in brain weight observed (Fig. 5 B & C)

Effect of DON on brain neurotransmitter levels in undernourished rats

To evaluate the impact of DON exposure on neurotransmitter homeostasis under undernourished conditions, the levels of DA, NE, 5-HT, and GABA were quantified in brain tissue samples. DON treatment resulted in significant alterations in neurotransmitter levels compared with control animals (Fig. 5D–G).

Undernourished rats exposed to DON at doses of 1 and 2.5 mg/kg exhibited a pronounced reduction in NE levels relative to both undernourished and DON alone (2.5mg/kg) groups. Similarly, DA, GABA, and 5-HT levels were significantly decreased in undernourished rats treated with DON, falling below those in the control, DON alone, and undernourished alone groups. Pretreatment of GSH significantly restored the concentrations toward control values (Fig. 5D–G). Notably, comparable patterns of neurotransmitter alterations and GSH-mediated amelioration were observed in both male and female rats, with no significant sex-dependent differences.

Effect of DON on Brain Cytokine Levels in Undernourished Rats

602 The effect of DON exposure on neuroinflammatory markers was evaluated by assessing
603 cytokine levels in brain tissue. DON treatment resulted in a significant upregulation of pro-
604 inflammatory cytokines, including interleukin (IL)-1β, IL-6, interferon-γ (IFN-γ), and IL-18,
605 compared with control animals. In undernourished rats exposed to DON, the levels of these
606 cytokines were further elevated in a dose-dependent manner, with the highest expression
607 observed at 2.5 mg/kg in both male and female rats (Fig. 6A, B, D, and F) compared to the
608 nourished DON alone group (2.5 mg/kg).
609 Pretreatment of GSH significantly attenuated DON-induced increases in pro-inflammatory
610 cytokine levels, bringing them closer to control values. In contrast, IL-10 levels were variably
611 reduced following DON exposure, particularly under undernourished conditions (Fig. 6C). A
612 marked downregulation of IL-12 was also observed in DON-treated undernourished rats,
613 compared to the nourished DON alone group (2.5 mg/kg) (Fig. 6E).
614 **Effect of DON on oxidative stress and antioxidant enzyme status in undernourished rats**
615 Oxidative stress parameters were evaluated in brain tissue to determine the impact of DON
616 exposure under undernourished conditions. DON administration resulted in a significant
617 increase in lipid peroxidation, as indicated by elevated MDA levels, in both (2.5mg/kg) DON
618 alone and undernourished DON-treated groups compared with control animals. Notably, the
619 increase in MDA levels was significantly more pronounced in undernourished rats exposed to
620 DON, particularly at the highest dose (2.5 mg/kg), in both male and female rats (Fig. 7A, B).
621 Pre-treatment with GSH significantly attenuated DON-induced lipid peroxidation in
622 undernourished rats, as evidenced by a marked reduction in MDA levels compared with
623 undernourished rats treated with DON alone (1 and 2.5 mg/kg) in both sexes. The reduction in
624 MDA levels in GSH-treated groups was also significantly different from that observed in DON-
625 alone groups (Fig. 7A, B).

In addition to enhanced lipid peroxidation, DON exposure resulted in a significant decline in the activities of key antioxidant enzymes, including SOD, GPX, and catalase CAT. This decrease was highly significant in undernourished rats treated with DON at 2.5 mg/kg compared with control and undernourished-alone groups (2.5 mg/kg). GSH pre-treatment in DON exposed undernourished rats significantly restored SOD, GPX, and CAT activities relative to DON treated undernourished male and female groups, indicating partial recovery of antioxidant defence capacity (Fig. 7C–E).

Undernourished alone rats exhibited significantly higher antioxidant enzyme activities compared with DON-treated undernourished rats, indicating that DON exposure markedly disrupted antioxidant homeostasis and further compromised redox balance under undernourished conditions. Collectively, these findings demonstrate that GSH supplementation attenuated DON-induced oxidative stress in undernourished rats, without markedly altering measured brain DON availability.

Effect of DON on total iron levels in the brain tissue of undernourished rats

Total iron levels were measured in brain tissue to assess alterations in iron homeostasis following DON exposure under undernourished conditions. DON treatment resulted in a significant increase in total brain iron levels compared with control animals. This increase was further accentuated in undernourished rats administered DON at doses of 1 and 2.5 mg/kg body weight significantly, when compared to the nourished DON alone group. Comparable patterns of iron accumulation were observed in both male and female rats (Fig. 7F).

Pretreatment of GSH significantly reduced total brain iron levels in undernourished rats treated with DON, bringing them closer to control values. Notably, the pattern of iron accumulation closely paralleled the extent of oxidative stress observed in these groups, as evidenced by elevated lipid peroxidation and compromised antioxidant defence. These findings indicate that

DON-induced oxidative imbalance under undernourished conditions is associated with disrupted iron homeostasis in brain tissue.

Oral administration of DON in undernourished conditions is associated with alterations in BBB tight junction proteins, ferroptosis and autophagy-associated pathways

Given the detection of DON in brain tissue following oral administration, the expression of key BBB tight junction proteins were examined to determine whether DON exposure under undernourished conditions was associated with alterations in BBB-associated molecular markers. Western blot analysis revealed that Claudin-5 (CLDN5), the principal tight junction protein governing BBB permeability, was significantly downregulated in undernourished rats exposed to DON at doses of 1 and 2.5 mg/kg (Fig. 8A). Undernourished DON treated male rats showed a more significant reduction in CLDN5 expression at 2.5 mg/kg, whereas female rats exhibited significant downregulation at 2.5 mg/kg compared with the undernourished or nourished DON alone group (2.5mg/kg)

In contrast, DON treatment alone did not significantly affect the expression of occludin or zonula occludens-1 (ZO-1) compared with controls. However, undernourished rats receiving DON displayed a marked, dose-dependent reduction in both occludin and ZO-1 expression relative to undernourished-alone and DON-treated (2.5 mg/kg) nourished groups (Fig. 8A). Pretreatment with GSH significantly restored the expression of CLDN5, occludin, and ZO-1 in DON-exposed undernourished rats, although protein levels did not fully return to control values.

To examine molecular changes associated with ferroptosis, the expression of glutathione peroxidase-4 (GPX4) and acyl-CoA synthetase long-chain family member-4 (ACSL4) was assessed. GPX4 levels were significantly reduced in undernourished rats treated with DON at all tested doses, with greater suppression observed at highest doses relative to undernourished-alone and DON-treated (2.5 mg/kg) nourished groups (Fig. 8B). GSH pretreatment partially

675 restored GPX4 expression however, the reults were more significant in male rats. Conversely,
676 acyl-CoA synthetase long-chain family member-4 (ACSL4), a pro-ferroptotic marker, was
677 markedly upregulated in DON-treated undernourished rats at both the tested doses (1-
678 2.5mg/kg), while its expression in nourished DON-alone and undernourished-alone groups
679 remained comparable to controls (Fig. 8B).
680 Neurotrophic support was also affected, as evidenced by a significant reduction in brain-
681 derived neurotrophic factor (BDNF) expression. Although modest decreases were observed in
682 DON-alone and undernourished-alone groups, a pronounced and significant downregulation
683 was evident in undernourished rats exposed to DON at 2.5 mg/kg compared to the nourished
684 DON group (2.5mg/kg) (Fig. 8B). GSH pretreatment significantly restored BDNF levels.
685 Finally, markers of autophagy-associated cell death were evaluated. Beclin-1 and LC3-II
686 protein levels were significantly elevated in DON-treated undernourished rats at 1 and 2.5
687 mg/kg compared to DON-treated nourished rats (2.5mg/kg) and undernourished alone,
688 indicating alteration in autophagy-associated signalling rather than definitive evidence of
689 increased autophagic flux or autophagy-dependent cell death. No caspase-3 expression was
690 detected in the evaluated samples (data not shown). GSH pretreatment significantly attenuated
691 the upregulation of Beclin-1 and LC3-II protein levels (Fig. 8B).
692 **Discussion**
693 DON is among the most frequently detected trichothecene mycotoxins in cereal based foods
694 worldwide, particularly in regions where food storage and regulatory oversight are suboptimal
695 (EFSA., 2017). While DON-associated gastrointestinal and immunotoxic effects are well
696 documented, its neurotoxic potential under conditions of nutritional deficiency has received
697 comparatively little attention.
698 Undernutrition remains highly prevalent in developing countries, where food quality may be
699 compromised and mycotoxin regulations are either insufficient or poorly enforced. Under such

conditions, exposure to DON through contaminated cereals may exert disproportionate adverse effects, particularly in children with ongoing brain development. The present study provides comprehensive evidence that undernutrition amplifies DON-induced neurobehavioral and neuropathological effects and is accompanied by changes in brain DON availability, BBB-associated proteins, oxidative stress, inflammatory mediators, iron homeostasis, and cell-stress pathways. The DON doses used in the present study (0.5, 1, and 2.5 mg/kg bw) were selected to represent graded toxicological exposure conditions previously employed in experimental rodent studies investigating DON-induced systemic reproductive and neurotoxic effects (Cao et al., 2020; Csikós et al., 2020; Cui et al., 2025; Ruan et al., 2024; Sprando et al., 2005; X. Zhang et al., 2025). Although the highest dose exceeds typical human dietary exposure levels, it was included to model severe contamination scenarios and to evaluate the impact of undernutrition on DON-induced neurotoxicity under conditions of enhanced susceptibility. Children and undernourished populations are considered particularly vulnerable to DON exposure due to higher cereal consumption relative to body weight and compromised physiological defences (Mishra et al., 2022; Tu et al., 2023). The undernourished rat model used in the present study was designed to reflect nutritionally vulnerable populations that are chronically exposed to food-borne mycotoxins such as DON, thereby mimicking real-world exposure scenarios prevalent in many developing regions. Behavioural impairments observed in the Morris water maze and elevated plus maze indicate that DON exposure under undernourished conditions significantly compromises learning, memory, and anxiety-related behaviours. Such cognitive deficits are consistent with previous reports linking trichothecene exposure and toxicity to the central nervous system dysfunction (Cui et al., 2025; Li et al., 2023; Su et al., 2025). Our study support's the recent findings of Yang et al. where DON-induced memory impairment following oral treatment of 2.5 mg/kg bw in mice (Yang et al., 2025). The greater severity of impairments in undernourished rats compared with DON-alone

725 animals suggests that nutritional stress critically modulates neurobehavioral outcomes. These
726 deficits were supported by histopathological evidence of dose-dependent neuronal loss and
727 enhanced neurodegeneration within the hippocampus, a brain region essential for learning and
728 memory. Earlier studies of Wang et al. and Cui et al have also shown that mice exposed to
729 DON exhibited neuronal shrinkage degeneration, neural tissue degeneration, in the cerebral
730 cortex and hippocampus, after exposing pigs and mice to 1.3 and 5 mg/kg/ bw DON,
731 respectively (Cui et al., 2025; Wang et al., 2020; X. Zhang et al., 2025). Importantly,
732 undernourished conditions are known to alter toxin bioavailability and antioxidant defences
733 which can effectively amplify internal exposure even at relatively low oral doses (Spencer &
734 Palmer, 2012), Consistent with this, pharmacokinetic analysis revealed substantially elevated
735 DON levels in brain tissues of undernourished animals compared with well-nourished
736 counterparts, supporting the notion that undernutrition facilitates DON absorption. Previous *in*
737 *vivo* studies have also reported that DON can reach the brain, supporting the relevance of brain
738 exposure to its neurotoxic effects (Sun et al., 2022). Alterations in brain neurotransmitter levels
739 further support the neurofunctional consequences of combined undernutrition and DON
740 exposure. The pronounced reduction in norepinephrine, serotonin, dopamine, and GABA
741 levels observed in undernourished DON-treated rats indicates dysregulation of monoaminergic
742 and inhibitory neurotransmission as compared to nourished DON treated rats. DON has
743 previously been shown to influence neurotransmitter signalling and appetite regulation through
744 central mechanisms (Prelusky et al., 1992; Wang et al., 2020; X. Zhang et al., 2025). Such
745 alterations may contribute to the observed behavioural phenotype, although the present study
746 does not establish a direct causal relationship between individual neurotransmitter changes and
747 behavioural outcomes. Neuro-inflammatory changes were also observed following DON
748 exposure under undernourished conditions. The marked changes in brain cytokine levels,
749 including increased IL-1β, IL-6, IFN-γ, and IL-18 together with altered IL-12 and IL-10

expression, are consistent with an inflammatory response. However, because cytokines were measured in whole-brain homogenates, their cellular sources cannot be determined from the present study; therefore, specific attribution to microglial or astrocytic activation should be avoided. DON is known to activate mitogen-activated protein kinase signalling and cytokine production in both peripheral and central tissues (Gaigé et al., 2013; C. Girardet et al., 2011; Clémence Girardet et al., 2011; X. Zhang et al., 2025). Chronic neuroinflammation can exacerbate neuronal damage and sensitize the brain to oxidative stress, particularly under conditions of nutritional insufficiency (Teleanu et al., 2022). The brain is particularly sensitive to oxidative stress caused by ROS, primarily because it utilises a significant amount of oxygen and contains substantial amounts of polyunsaturated fatty acids. When ROS are generated, they can interfere with the brain's ability to regulate iron levels, often leading to a buildup of iron. This excess iron can worsen oxidative stress and may play a role in neurodegenerative processes (Gao et al., 2025; Trofin et al., 2025). Consistent with this inflammatory profile, DON exposure resulted in pronounced oxidative stress in the brain, as evidenced by increased lipid peroxidation and impaired antioxidant defence. Elevation of malondialdehyde levels, together with suppression of SOD, CAT, and GPX activities, was most pronounced in undernourished rats exposed to higher DON doses when compared to the DON-treated nourished-alone group. Oxidative stress is a well-established mechanism of DON toxicity (Mishra, Dwivedi, et al., 2014) and undernutrition is known to weaken endogenous antioxidant systems, thereby increasing susceptibility to redox imbalance. Under conditions of toxicant exposure, cells typically activate adaptive mechanisms to preserve protein and metabolic homeostasis and maintain essential housekeeping functions. Previous studies have shown that mycotoxin stress induces selective prioritization of cellular homeostasis pathways as a protective response against toxic injury (Sun et al., 2019). Such stress may promote alterations in cellular homeostasis and increase vulnerability to regulated cell-death pathways. Notably,

oxidative stress was accompanied by significant iron accumulation in the brain of undernourished DON-treated rats. The concurrent downregulation of GPX4 and upregulation of ACSL4, together with increased lipid peroxidation and total iron, are consistent with ferroptosis-associated molecular changes .(Benarroch, 2023). However, total iron accumulation does not establish an increase in the labile iron pool or iron-dependent cell death, and GPX4/ACSL4 changes are not specific enough to demonstrate ferroptosis independently. Therefore, the present findings should be interpreted as evidence of a ferroptosis-associated response rather than definitive proof that ferroptosis is the cause of neuronal injury. Functional studies using ferroptosis-specific inhibitors or complementary mechanistic approaches would be required to establish causality. Reduced BDNF expression may also be relevant to the observed neurobehavioral phenotype, but the present data do not demonstrate that BDNF reduction mediates the behavioural effects. Changes in the expression of BBB-associated proteins was another prominent finding. Reduced CLDN5, occludin, and ZO-1 expression in DON-exposed undernourished rats is consistent with altered BBB integrity. However, tight-junction protein expression alone does not directly quantify BBB permeability. The higher brain DON concentrations observed in the pharmacokinetic experiment provide complementary evidence of altered brain exposure, but without concurrent plasma measurements or a direct permeability assay, the contribution of BBB transfer cannot be isolated. Interestingly, although female undernourished rats exhibited greater neuronal loss and a more pronounced reduction in CLDN5 expression compared with males, these differences were not reflected in the behavioural assessments. Behavioural outcomes in neurotoxicity studies may not always directly correlate with the extent of cellular or molecular damage, particularly during early or subclinical stages of injury. It is possible that compensatory neuroadaptive responses, sex-specific differences in neural circuit resilience, or variability in behavioral sensitivity may have masked overt sex-dependent behavioral differences despite

greater histopathological alterations in females. Similar dissociations between molecular injury and behavioral manifestations have been reported in previous neurotoxicity studies (Arezzo et al., 2011) but these possibilities remain speculative and require further investigation. . GSH supplementation partially restored the expression of several tight-junction proteins, suggesting that redox status may be associated with the observed changes in BBB-related markers. Alterations in Beclin-1 and LC3 expression, particularly at higher doses, also suggest changes in autophagy-associated markers under undernourished conditions. Although autophagy is initially a protective stress response, its excessive activation can promote neuronal loss. As DON-induced autophagy has already been well documented (Mishra et al., 2024; X. Zhang et al., 2025), the present study focused on evaluating key endpoint markers rather than upstream signalling pathways. The relationship between ferroptosis-associated and autophagy-associated responses therefore remains an important hypothesis for future investigation rather than a demonstrated synergistic mechanism in the present study. Partial normalisation of these markers following GSH supplementation suggests that oxidative stress might play a role in driving autophagy-associated cell death. Recent work published by Zhang et al. (H. Zhang et al., 2025) has highlighted the capacity of glutathione to detoxify DON through the formation of DON-GSH conjugate, resulting in reduced cytotoxicity and preservation of intestinal barrier integrity in vitro. While that study primarily focused on chemical biotransformation and cellular outcomes, the present *in vivo* findings extend these observations by demonstrating that GSH supplementation was associated with partial attenuation of several DON-induced alterations under nutritional stress. In the present model, GSH reduced oxidative stress and partially ameliorated neuroinflammatory, BBB-associated, and neuronal changes without markedly altering measured brain DON availability. These findings are compatible with a protective role of GSH through redox regulation and/or detoxification-related mechanisms; however, the present study does not distinguish between these mechanisms. Further

pharmacokinetic and biochemical studies would be required to determine the relative contribution of DON-GSH conjugation to the observed protection.

From a food-safety perspective, these findings support consideration of nutritional status as a potential susceptibility factor in DON risk assessment. The present study does not establish a new permissible exposure limit or demonstrate that currently established regulatory limits are insufficient for undernourished populations. Rather, the findings raise the possibility that nutritional status may modify susceptibility to DON-associated neurotoxicity and therefore warrants consideration in future risk-assessment frameworks, particularly when evaluating vulnerable populations. In conclusion, the present study demonstrates that undernutrition increases susceptibility to DON-induced neurotoxicity and is accompanied by increased brain DON availability, altered expression of BBB tight-junction proteins, oxidative stress, neuroinflammatory changes, iron accumulation, neuronal degeneration, and changes in ferroptosis- and autophagy-associated markers. Future studies incorporating plasma and brain pharmacokinetics, direct BBB permeability measurements, flux-based autophagy assays, and pathway-specific inhibition of ferroptosis and autophagy will be important for defining the causal relationships among these processes. From a public health perspective, these findings underscore the need to incorporate nutritional status into food safety regulations and mycotoxin risk assessments, particularly in regions where undernutrition and dietary mycotoxin exposure frequently coexist. This approach is especially critical for vulnerable populations, including children, for whom chronic exposure during critical developmental windows may have long-term consequences for brain health and cognitive function.

CRediT authorship contribution statement

Sakshi Mishra: Writing –original draft, Investigation, Conceptualisation, Formal analysis, Funding acquisition. **Divyansh Sharma:** Methodology, Investigation. **Gaurav Jha:** Methodology, Investigation. **Bhawna Tomar:** Methodology, Investigation. **Sonam**

Kanchan: Methodology, Investigation. **Anuj Kumar:** Methodology, Investigation, Visualisation. **Radhika Kapoor:** Conceptualisation. **Sristi Agarwal:** Methodology, Investigation, Visualisation. **Rabi Bhatta:** Resources, Methodology, **Shubha Shukla:** Resources, Methodology, **Srikanta Kumar Rath:** Writing – review & editing, Supervision, Resources, Methodology, Conceptualisation.

Declaration of Competing Interests: The authors declare that they have no known competing financial interests or personal relationships that could have appeared to influence the work reported in this paper.

Funding: This work was supported by the Department of Science and Technology (DST), Government of India, under the Women Scientist Scheme (WOS-A) [Reference No. SR/WOS-A/LS-114/2019]. The CSIR-Central Drug Research Institute (CSIR-CDRI) communication number for this manuscript is 14/2026/SKR

Declaration of Generative AI and AI-assisted technologies in the writing process

During the preparation of this work, the author(s) used (Scispace) to improve the language and readability of the manuscript. After using this tool/service, the author(s) reviewed and edited the content as needed and take(s) full responsibility for the content of the publication.

Appendix A. Supplementary data

Supplementary material: **Table S1.** Initial body weight, final body weight, body length, abdominal circumference (AC), thoracic circumference (TC), AC/TC ratio, body mass index (BMI), Lee index, after 28 days of model development for undernutrition in male and female rats. **Table S2:** Haematological parameters of *Wistar* rats after 28 days of a 50% food-restricted diet. **Table S3.** Biochemical parameters of *Wistar* rats after 28 days of a 50% food-restricted diet. **Table S4.** Initial body weight, final body weight, body length, abdominal circumference (AC), thoracic circumference (TC), AC/TC ratio, body mass index (BMI), Lee index, after 28 days of DON dosing in undernourished male and female rats. **Table S5:** Haematological parameters of *Wistar* rats after 28 days of DON exposure in undernourished

rats. **Table S6**: Biochemical parameters of *Wistar* rats after DON exposure in undernourished rats.

Data availability

Data will be made available on request.

References

Arezzo, J. C., Litwak, M. S., & Zotova, E. G. (2011). Correlation and dissociation of electrophysiology and histopathology in the assessment of toxic neuropathy. *Toxicol Pathol*, *39*(1), 46-51. https://doi.org/10.1177/0192623310390231

Bañuls, C., de Marañon, A. M., Veses, S., Castro-Vega, I., López-Domènech, S., Salom-Vendrell, C.,…Hernández-Mijares, A. (2019). Malnutrition impairs mitochondrial function and leukocyte activation. *Nutr J*, *18*(1), 89. https://doi.org/10.1186/s12937-019-0514-7

Behrens, M., Huwel, S., Galla, H. J., & Humpf, H. U. (2015). Blood-Brain Barrier Effects of the Fusarium Mycotoxins Deoxynivalenol, 3 Acetyldeoxynivalenol, and Moniliformin and Their Transfer to the Brain. *PLoS One*, *10*(11), e0143640. https://doi.org/10.1371/journal.pone.0143640

Benarroch, E. (2023). What Is the Role of Ferroptosis in Neurodegeneration? *Neurology*, *101*(7), 312-319. https://doi.org/10.1212/wnl.0000000000207730

Bernardis, L. L., & Patterson, B. D. (1968). Correlation between 'Lee index' and carcass fat content in weanling and adult female rats with hypothalamic lesions. *J Endocrinol*, *40*(4), 527-528. https://doi.org/10.1677/joe.0.0400527

Cao, L., Jiang, Y., Zhu, L., Xu, W., Chu, X., Zhang, Y.,…Wang, X. (2021). Deoxynivalenol Induces Caspase-8-Mediated Apoptosis through the Mitochondrial Pathway in Hippocampal Nerve Cells of Piglet. *Toxins (Basel)*, *13, 73*(2). https://doi.org/10.3390/toxins13020073

Cao, Z., Huang, W., Sun, Y., & Li, Y. (2020). Deoxynivalenol induced spermatogenesis disorder by blood-testis barrier disruption associated with testosterone deficiency and inflammation in mice. *Environmental Pollution*, *264*, 114748. https://doi.org/https://doi.org/10.1016/j.envpol.2020.114748

Cesani, M. F., Orden, B., Zucchi, M., Muñe, M. C., Oyhenart, E. E., & Pucciarelli, H. M. (2003). Effect of undernutrition on the cranial growth of the rat. An intergenerational study. *Cells Tissues Organs*, *174*(3), 129-135. https://doi.org/10.1159/000071153

Claeys, L., Romano, C., De Ruyck, K., Wilson, H., Fervers, B., Korenjak, M.,…Safety, F. (2020). Mycotoxin exposure and human cancer risk: A systematic review of epidemiological studies. *19*(4), 1449-1464.

Csikós, V., Varró, P., Bódi, V., Oláh, S., Világi, I., & Dobolyi, A. (2020). The mycotoxin deoxynivalenol activates GABAergic neurons in the reward system and inhibits feeding and maternal behaviours. *Arch Toxicol*, *94*(9), 3297-3313. https://doi.org/10.1007/s00204-020-02791-6

Cui, Y., Okyere, S. K., Guan, H., Hua, Z., Deng, Y., Deng, H., & Deng, J. (2025). Ablation of Gut Microbiota Alleviates DON-Induced Neurobehavioral Abnormalities and Brain Damage in Mice. *17*(3), 144. https://www.mdpi.com/2072-6651/17/3/144

Deng, Y., You, L., Wang, X., Wu, W., Kuca, K., Wu, Q., & Wei, W. (2023). Deoxynivalenol: Emerging Toxic Mechanisms and Control Strategies, Current and Future Perspectives. *J Agric Food Chem*, *71*(29), 10901-10915. https://doi.org/10.1021/acs.jafc.3c02020

EFSA. (2017). Risks to human and animal health related to the presence of deoxynivalenol and its acetylated and modified forms in food and feed. *EFSA Journal*, *15(9)*(4718), 345.

Eskola, M., Kos, G., Elliott, C. T., Hajšlová, J., Mayar, S., & Krska, R. (2019). Worldwide contamination of food-crops with mycotoxins: Validity of the widely cited 'FAO estimate' of 25%. *Critical Reviews in Food Science and Nutrition*, 1-17. https://doi.org/10.1080/10408398.2019.1658570

Ferreira-Paes, T., Seixas-Costa, P., & Almeida-Amaral, E. E. (2021). Validation of a Feed Protocol in a Mouse Model That Mimics Marasmic Malnutrition. *Front Vet Sci*, *8*, 757136. https://doi.org/10.3389/fvets.2021.757136

Firmenich, D. (2024). *World Mycotoxin Survey The Global Threat January – December 2024*. https://pages-anh.dsm.com/rs/944-XYO-531/images/REP_MTXsurvey_Q4_0125_62309_FINAL.pdf?version=0&mkt_tok=OTQ0LVhZTy

01MzEAAAGYwVgdUrQjxyGHrheXwZjwYSI_MnT5J3bAg1h5F38d09RdDQaqzvXMrOmGz-iCl_BtvNCZVE9kuo3YDNQxhSSUAzX-Hio7LD1tEqB6QqF42Q
Gaigé, S., Bonnet, M. S., Tardivel, C., Pinton, P., Trouslard, J., Jean, A.,…Dallaporta, M. J. N. (2013). c-Fos immunoreactivity in the pig brain following deoxynivalenol intoxication: focus on NUCB2/nesfatin-1 expressing neurons. *34*, 135-149.
Gao, Q., Zhou, Y., Chen, Y., Hu, W., Jin, W., Zhou, C.,…Lin, W. (2025). Role of iron in brain development, aging, and neurodegenerative diseases. *Ann Med*, *57*(1), 2472871. https://doi.org/10.1080/07853890.2025.2472871
Girardet, C., Bonnet, M. S., Jdir, R., Sadoud, M., Thirion, S., Tardivel, C.,…Troadec, J. D. (2011). Central inflammation and sickness-like behavior induced by the food contaminant deoxynivalenol: a PGE2-independent mechanism. *Toxicol Sci*, *124*(1), 179-191. https://doi.org/10.1093/toxsci/kfr219
Girardet, C., Bonnet, M. S., Jdir, R., Sadoud, M., Thirion, S., Tardivel, C.,…Mounien, L. J. P. o. (2011). The food-contaminant deoxynivalenol modifies eating by targeting anorexigenic neurocircuitry. *6*(10), e26134.
Gruber-Dorninger, C., Jenkins, T., & Schatzmayr, G. J. T. (2019). Global mycotoxin occurrence in feed: A ten-year survey. *11*(7), 375.
Hardikar, A. A., Satoor, S. N., Karandikar, M. S., Joglekar, M. V., Puranik, A. S., Wong, W.,…Yajnik, C. S. (2015). Multigenerational Undernutrition Increases Susceptibility to Obesity and Diabetes that Is Not Reversed after Dietary Recuperation. *Cell Metab*, *22*(2), 312-319. https://doi.org/10.1016/j.cmet.2015.06.008
Jia, B., Lin, H., Yu, S., Liu, N., Yu, D., & Wu, A. (2023). Mycotoxin deoxynivalenol-induced intestinal flora disorders, dysfunction and organ damage in broilers and pigs. *J Hazard Mater*, *451*, 131172. https://doi.org/https://doi.org/10.1016/j.jhazmat.2023.131172
Kraeuter, A.-K., Guest, P. C., & Sarnyai, Z. (2019). The Elevated Plus Maze Test for Measuring Anxiety-Like Behavior in Rodents. In P. C. Guest (Ed.), *Pre-Clinical Models: Techniques and Protocols* (pp. 69-74). Springer New York. https://doi.org/10.1007/978-1-4939-8994-2_4
Li, N., Yao, C. Y., Diao, J., Liu, X. L., Tang, E. J., Huang, Q. S.,…Cai, T. J. (2023). The role of MAPK/NF-κB-associated microglial activation in T-2 toxin-induced mouse learning and memory impairment. *Food Chem Toxicol*, *174*, 113663. https://doi.org/10.1016/j.fct.2023.113663
Liu, Y., Lu, Y., Wang, L., Chang, F., & Yang, L. J. F. c. (2016). Occurrence of deoxynivalenol in wheat, Hebei Province, China. *197*, 1271-1274.
Locatelli, S., Scarpino, V., Lanzanova, C., Romano, E., & Reyneri, A. (2022). Multi-Mycotoxin Long-Term Monitoring Survey on North-Italian Maize over an 11-Year Period (2011-2021): The Co-Occurrence of Regulated, Masked and Emerging Mycotoxins and Fungal Metabolites. *Toxins (Basel)*, *14*(8). https://doi.org/10.3390/toxins14080520
Lombard, M. J. (2014). Mycotoxin exposure and infant and young child growth in Africa: what do we know? *Annals of nutrition & metabolism*, *64 Suppl 2*, 42-52. https://doi.org/10.1159/000365126
Mishra, S., Dixit, S., Dwivedi, P. D., Pandey, H. P., & Das, M. (2014). Influence of temperature and pH on the degradation of deoxynivalenol (DON) in aqueous medium: Comparative cytotoxicity of DON and degraded product. *Food Additives & Contaminants: Part A*, *31*(1), 121-131.
Mishra, S., Dwivedi, P. D., Pandey, H. P., & Das, M. (2014). Role of oxidative stress in Deoxynivalenol induced toxicity. *Food and Chemical Toxicology*, *72*, 20-29. https://doi.org/10.1016/j.fct.2014.06.027
Mishra, S., Kapoor, R., Sushma, Kanchan, S., Jha, G., Sharma, D.,…Rath, S. K. (2024). Deoxynivalenol Induces Drp-1-Mediated Mitochondrial Dysfunction via Elevating Oxidative Stress. *Chem Res Toxicol*, *37*(7), 1139-1154. https://doi.org/10.1021/acs.chemrestox.4c00066
Mishra, S., Srivastava, S., Dewangan, J., Divakar, A., & Kumar Rath, S. (2022). Global occurrence of deoxynivalenol in food commodities and exposure risk assessment in humans in the last

decade: a survey. *Critical Reviews in Food Science and Nutrition*, *60*(8), 1346-1374. https://doi.org/10.1080/10408398.2019.1571479

Mishra, S. K., Singh, S., Shukla, S., & Shukla, R. J. N. I. (2018). Intracerebroventricular streptozotocin impairs adult neurogenesis and cognitive functions via regulating neuroinflammation and insulin signaling in adult rats. *113*, 56-68.

Nair, A. B., & Jacob, S. (2016). A simple practice guide for dose conversion between animals and human. *J Basic Clin Pharm*, *7*(2), 27-31. https://doi.org/10.4103/0976-0105.177703

Pestka, J. J. (2010). Deoxynivalenol-induced proinflammatory gene expression: mechanisms and pathological sequelae. *Toxins (Basel)*, *2*(6), 1300-1317.

Prelusky, D. B., Hartin, K. E., & Trenholm, H. L. (1990). Distribution of deoxynivalenol in cerebral spinal fluid following administration to swine and sheep. *J Environ Sci Health B*, *25*(3), 395-413. https://doi.org/10.1080/03601239009372697

Prelusky, D. B., Yeung, J. M., Thompson, B. K., & Trenholm, H. L. (1992). Effect of deoxynivalenol on neurotransmitters in discrete regions of swine brain. *Archives of Environmental Contamination and Toxicology*, *22*(1), 36-40. https://doi.org/10.1007/BF00213300

Quiróz-González, S., Escartín-Pérez, R. E., Paz-Bermudez, F., Segura-Alegría, B., Reyes-Legorreta, C., Guadarrama-Olmos, J. C.,…Jiménez-Estrada, I. (2013). Endogenous content and release of [(3)H]-GABA and [(3)H]-glutamate in the spinal cord of chronically undernourished rat. *Neurochem Res*, *38*(1), 23-31. https://doi.org/10.1007/s11064-012-0881-3

Razafimanjato, H., Benzaria, A., Taïeb, N., Guo, X. J., Vidal, N., Di Scala, C.,…Maresca, M. (2011). The ribotoxin deoxynivalenol affects the viability and functions of glial cells. *Glia*, *59*(11), 1672-1683.

Reis, J., & Spencer, P. S. (2024). An introduction to environmental neurotoxicology: Lessons from a clinical perspective. *Journal of the Neurological Sciences*, *463*, 123108. https://doi.org/https://doi.org/10.1016/j.jns.2024.123108

Ruan, Y.-B., Liu, X.-H., Jiang, J.-Z., Nie, T., & Ma, J. J. S. o. T. T. E. (2024). Leydig cells pyroptosis in testis mediates deoxynivalenol-induced male reproductive toxicity in mice. *954*, 176432.

Siddiqui, F., Salam, R. A., Lassi, Z. S., & Das, J. K. (2020). The Intertwined Relationship Between Malnutrition and Poverty. *Front Public Health*, *8*, 453. https://doi.org/10.3389/fpubh.2020.00453

Silva, M. V., Pante, G. C., Romoli, J. C. Z., de Souza, A. P. M., Rocha, G., Ferreira, F. D.,…Machinski, M., Jr. (2018). Occurrence and risk assessment of population exposed to deoxynivalenol in foods derived from wheat flour in Brazil. *Food Addit Contam Part A Chem Anal Control Expo Risk Assess*, *35*(3), 546-554. https://doi.org/10.1080/19440049.2017.1411613

Spencer, P. S., & Palmer, V. S. (2012). Interrelationships of undernutrition and neurotoxicity: food for thought and research attention. *Neurotoxicology*, *33*(3), 605-616. https://doi.org/10.1016/j.neuro.2012.02.015

Sprando, R. L., Collins, T. F., Black, T. N., Olejnik, N., Rorie, J. I., Eppley, R. M.,…Toxicology, C. (2005). Characterization of the effect of deoxynivalenol on selected male reproductive endpoints. *43*(4), 623-635.

Stoev, S. D. (2024). Food security, underestimated hazard of joint mycotoxin exposure and management of the risk of mycotoxin contamination. *Food Control*, *159*, 110235. https://doi.org/https://doi.org/10.1016/j.foodcont.2023.110235

Su, S.-Q., Xiong, G.-Y., Yao, C.-Y., Liu, X.-L., Xia, Y.-Y., Long, J.-Y.,…Cai, T.-J. (2025). T-2 toxin-induced spatial learning and memory impairment in mice via the gut-brain axis and the intervening effects of resveratrol. *Ecotoxicol Environ Saf*, *302*, 118623. https://doi.org/https://doi.org/10.1016/j.ecoenv.2025.118623

Sun, Y., Jiang, J., Mu, P., Lin, R., Wen, J., & Deng, Y. (2022). Toxicokinetics and metabolism of deoxynivalenol in animals and humans. *Arch Toxicol*, *96*(10), 2639-2654. https://doi.org/10.1007/s00204-022-03337-8

Sun, Y., Wen, J., Chen, R., & Deng, Y. (2019). Variable protein homeostasis in housekeeping and non-housekeeping pathways under mycotoxins stress. *Sci Rep*, *9*(1), 7819. https://doi.org/10.1038/s41598-019-44305-0

Tchonkouang, R. D., Onyeaka, H., & Nkoutchou, H. (2024). Assessing the vulnerability of food supply chains to climate change-induced disruptions. *Science of the Total Environment*, *920*, 171047. https://doi.org/https://doi.org/10.1016/j.scitotenv.2024.171047

Teleanu, D. M., Niculescu, A.-G., Lungu, I. I., Radu, C. I., Vladâcenco, O., Roza, E.,…Teleanu, R. I. (2022). An Overview of Oxidative Stress, Neuroinflammation, and Neurodegenerative Diseases. *23*(11), 5938. https://www.mdpi.com/1422-0067/23/11/5938

Tiwari, V., Mishra, A., Singh, S., Mishra, S. K., Sahu, K. K., Kulkarni, M. J.,…Shukla, S. J. B. R. (2021). Protriptyline improves spatial memory and reduces oxidative damage by regulating NFκB-BDNF/CREB signaling axis in streptozotocin-induced rat model of Alzheimer's disease. *1754*, 147261.

Trofin, D.-M., Sardaru, D.-P., Trofin, D., Onu, I., Tutu, A., Onu, A.,…Matei, D. V. (2025). Oxidative Stress in Brain Function. *14*(3), 297. https://www.mdpi.com/2076-3921/14/3/297

Tu, Y., Liu, S., Cai, P., & Shan, T. (2023). Global distribution, toxicity to humans and animals, biodegradation, and nutritional mitigation of deoxynivalenol: A review. *Compr Rev Food Sci Food Saf*, *22*(5), 3951-3983. https://doi.org/10.1111/1541-4337.13203

Vázquez-Mendoza, E., Rodríguez-Torres, E. E., López-García, K., Hinojosa-Rodríguez, C. X., & Jiménez-Estrada, I. (2017). Differential effect of chronic undernutrition on the fiber type composition of fascicles in the extensor digitorum longus muscles of the rat. *Acta Histochem*, *119*(4), 364-371. https://doi.org/10.1016/j.acthis.2017.03.005

Wang, X., Chen, X., Cao, L., Zhu, L., Zhang, Y., Chu, X.,…Wu, J. (2020). Mechanism of deoxynivalenol-induced neurotoxicity in weaned piglets is linked to lipid peroxidation, dampened neurotransmitter levels, and interference with calcium signaling. *Ecotoxicol Environ Saf*, *194*, 110382. https://doi.org/10.1016/j.ecoenv.2020.110382

Wang, X., Fan, M., Chu, X., Zhang, Y., Rahman, S. u., Jiang, Y.,…Wu, J. (2018). Deoxynivalenol induces toxicity and apoptosis in piglet hippocampal nerve cells via the MAPK signaling pathway. *Toxicon*, *155*, 1-8. https://doi.org/https://doi.org/10.1016/j.toxicon.2018.09.006

Watson, S., Gong, Y. Y., & Routledge, M. (2017). Interventions targeting child undernutrition in developing countries may be undermined by dietary exposure to aflatoxin. *Crit Rev Food Sci Nutr*, *57*(9), 1963-1975. https://doi.org/10.1080/10408398.2015.1040869

Weaver, A. C., Weaver, D. M., Adams, N., & Yiannikouris, A. J. T. (2021). Co-occurrence of 35 mycotoxins: A seven-year survey of corn grain and corn silage in the United States. *13*(8), 516.

WHO. (2016). *World Health Organisation , Press Release N° 242*. Retrieved from https://www.iarc.fr/wp-content/uploads/2018/07/pr242_E.pdf

Yang, L.-N., Li, T., Liu, Y., Nüssler, A. K., Liu, L., Xu, Q.,…Yang, W. (2025). Memory impairment mediated by deoxynivalenol via the BLA-PrL circuit. *J Hazard Mater*, *496*, 139172. https://doi.org/https://doi.org/10.1016/j.jhazmat.2025.139172

Zhang, H., Zheng, S., Zuo, Y., Yu, Y., Yang, J., & Tang, Y. (2025). A novel glutathione-conjugates of deoxynivalenol biotransformation in vitro and the cytotoxic properties evaluation. *Food Research International*, *214*, 116634. https://doi.org/https://doi.org/10.1016/j.foodres.2025.116634

Zhang, X., Li, S., Guo, H., Wang, J., Wen, T., Wang, X., & Wang, C. (2025). Deoxynivalenol triggers pyroptosis in mouse hippocampal neurons by activating oxidative stress and interfering with neurotransmitter release. *J Hazard Mater*, *496*, 139343. https://doi.org/https://doi.org/10.1016/j.jhazmat.2025.139343

Legends to Figures

Figure 1 (A). Evaluation of the weight of rat submitted or not to experimental undernutrition. Percentage of weight gained at the end of the experiment for male rats. (C) Female rats. At the end of the experiment (day 36), the weight gain percentage was analyzed by dividing the final weight (day 36) by the initial weight (day 8) of the rats. Evaluation of phenotypic markers of rats submitted or not to experimental undernutrition. Body measurements were calculated at days 1, 6, 16, and 28 after diet introduction (B) Body mass index of male rats. (D) Body mass index of female rats. Evaluation of the body weight of rat orally exposed to different doses of DON/GSH in undernourished conditions (E). Body weight gained during the experiment for male rats (F) Female rats. Rats were weighed weekly till the end of experiment. G) Body mass index of male rats. (H) Body mass index of female rats. Data presented as mean ± SEM, *p < 0.05, **p < 0.01, ***p < 0.001; all comparisons against Group I. #p < 0.05, ##p < 0.01, ###p < 0.001, and ****p < 0.0001; all comparisons against Group II.

Figure 2. DON-induced anxiety were evaluated on day 60, (A) Elevated plus maze test was performed to evaluate the anxiety-like behaviour, and the bar graph shows the time spent in an open arm. Comparisons were made on the basis of the two-way analysis of variance (ANOVA) followed by the Dunnett's multiple comparison test, using Graph Pad Instat software (Graph Pad Software Inc. CA, USA). Spatial learning and memory ability of DON treated undernourished rats were evaluated with the Morris water maze test. (B) time spent in target quadrant in probe trials. (C) Latency to find a hidden platform in the water maze over three consecutive days of training, (D) Mean of path length in session trials, (E) Track plots; Representative search strategy of rats. Comparisons were made on the basis of the Two-way analysis of variance (ANOVA) followed by the Bonferroni's multiple comparison test, using Graph Pad Instat software (Graph Pad Software Inc. CA, USA). All data are expressed as Mean ± SEM (n = 10). *p < 0.05, **p < 0.01, ***p < 0.001 all comparisons against control. $^{\#}$p < 0.05, $^{\#\#}$p < 0.01, $^{\#\#\#}$p < 0.001 all comparisons against DON. $^{\$}$p < 0.05, $^{\$\$}$p < 0.01, $^{\$\$\$}$p < 0.001 all comparisons against UN. $^{@}$p < 0.05, $^{@@}$p < 0.01, $^{@@@}$p < 0.001 all comparisons against DON (1mg/kg)+UN.

Figure 3. Histology of rat hippocampus region. Photomicrograph of Wistar rat hippocampus showing healthy neuron (black arrow) and degenerated neuron (red arrow) stained with Cresyl violet (magnification, 40x). Hippocampus; Rat, neurons of granular layer, Control group: showing normal histological architecture; granular neurons (black arrow). DON (alone and in undernourished conditions) treated group: showing degeneration/ necrosis of sporadic granular neurons (red arrow). (scale bar 50 µm)

Figure 4. Fluoro-Jade® B staining of the cortex. Fluoro-Jade® B (FJB) staining showed distribution of damaged neurons throughout all layers of the cortex in DON treated undernourished male and female rats (A-D). All data are expressed as Mean ± SEM (n = 10). *p < 0.05, **p < 0.01, ***p < 0.001 all comparisons against control. $^{\#}$p < 0.05, $^{\#\#}$p < 0.01, $^{\#\#\#}$p < 0.001 all comparisons against DON. $^{\$}$p < 0.05, $^{\$\$}$p < 0.01, $^{\$\$\$}$p < 0.001 all comparisons against UN (undernourishment). $^{@}$p < 0.05, $^{@@}$p < 0.01, $^{@@@}$p < 0.001 all comparisons against DON (1mg/kg)+UN.

Figure 5. (A) Time-dependent concentrations of DON in brain tissue following oral administration. Brain tissue was collected at the specified post-dose time points (15 min, 30 min, 1 h) and DON concentrations were quantified using LC–MS/MS Comparisons were made on the basis of the one-way analysis of variance (ANOVA) followed by the Bonferroni multiple comparison test, using Graph Pad Instat software (Graph Pad Software Inc. CA, USA). All data are expressed as Mean ± SEM (n = 3). *** P ≤ 0.001 vs DON. (B) Brain weight of male and (C) female rats. (D-G). Effect of oral administration of DON on the brain neurotransmitters (NE, 5-HT, DA, GABA), levels at the end of the 65th day of duration on male and female rats. All data are expressed as Mean ± SEM (n=. *p < 0.05, **p < 0.01, ***p < 0.001 all comparisons against control. $^{\#}$p < 0.05, $^{\#\#}$p < 0.01, $^{\#\#\#}$p < 0.001 all comparisons against DON. $^{\$}$p < 0.05, $^{\$\$}$p < 0.01, $^{\$\$\$}$p < 0.001, all comparisons against UN (undernourishment). $^{@}$p < 0.05, $^{@@}$p < 0.01, $^{@@@}$p < 0.001 all comparisons against DON (1mg/kg)+UN.

Figure 6. Effect of oral administration of DON on undernourished and nourished male and female rats on the cytokine levels at the end of the 65th day (A-F). Data are shown as means ± SD, N = 5 rats/group, Comparisons were made based on the two-way analysis of variance (ANOVA) followed by the Dunnett's multiple comparison test, using Graph Pad Instat software (Graph Pad Software Inc. CA, USA). All data are expressed as Mean ± SEM (n=. *p < 0.05, **p < 0.01, ***p < 0.001 all comparisons against control. $^{\#}$p < 0.05, $^{\#\#}$p < 0.01, $^{\#\#\#}$p < 0.001 all comparisons against DON. $^{\$}$p < 0.05, $^{\$\$}$p < 0.01, $^{\$\$\$}$p < 0.001, all comparisons against UN (undernourishment). $^{@}$p < 0.05, $^{@@}$p < 0.01, $^{@@@}$p < 0.001 all comparisons against DON (1mg/kg)+UN.

Figure 7. Effect of oral administration of DON on undernourished and nourished male and female rats on the MDA and antioxidant enzyme status at the end of the 65th day (A-F). Comparisons were made based on the two-way analysis of variance (ANOVA) followed by the Dunnett's multiple comparison test, using Graph Pad Instat software (Graph Pad Software Inc. CA, USA). All data are expressed as Mean ± SEM, N = 5 rats/group, (n=. *p < 0.05, **p < 0.01, ***p < 0.001 all comparisons against control. $^{\#}$p < 0.05, $^{\#\#}$p < 0.01, $^{\#\#\#}$p < 0.001 all comparisons against DON. $^{\$}$p < 0.05, $^{\$\$}$p < 0.01, $^{\$\$\$}$p < 0.001, all comparisons against UN (undernourishment). $^{@}$p < 0.05, $^{@@}$p < 0.01, $^{@@@}$p < 0.001 all comparisons against DON (1mg/kg)+UN.

Figure. 8. Effect of oral administration of DON and GSH on undernourished rats. (A) Immunoblots of CLDN5, Occludin, ZO-1, GPX4, ACSL4, BDNF, Beclin-1, LC3 of brain tissue. β-Actin as the loading control and **(B)** densitometry was done using ImageJ. All data are expressed as Mean ± SEM (n=5) *p < 0.05, **p < 0.01, ***p < 0.001, all comparisons against control. $^{\#}p < 0.05$, $^{\#\#}p < 0.01$, $^{\#\#\#}p < 0.001$ all comparisons against DON. $^{\$}p < 0.05$, $^{\$\$}p < 0.01$, $^{\$\$\$}p < 0.001$, all comparisons against UN (undernourishment). $^{@}p < 0.05$, $^{@@}p < 0.01$, $^{@@@}p < 0.001$ all comparisons against DON (1mg/kg)+UN.

Legends to Table-

Table1: The table shows the optimised MS parameters of analyte, IS and instrument.

Table2: Weight-for-age relationship (WA) Value for male and female rats.

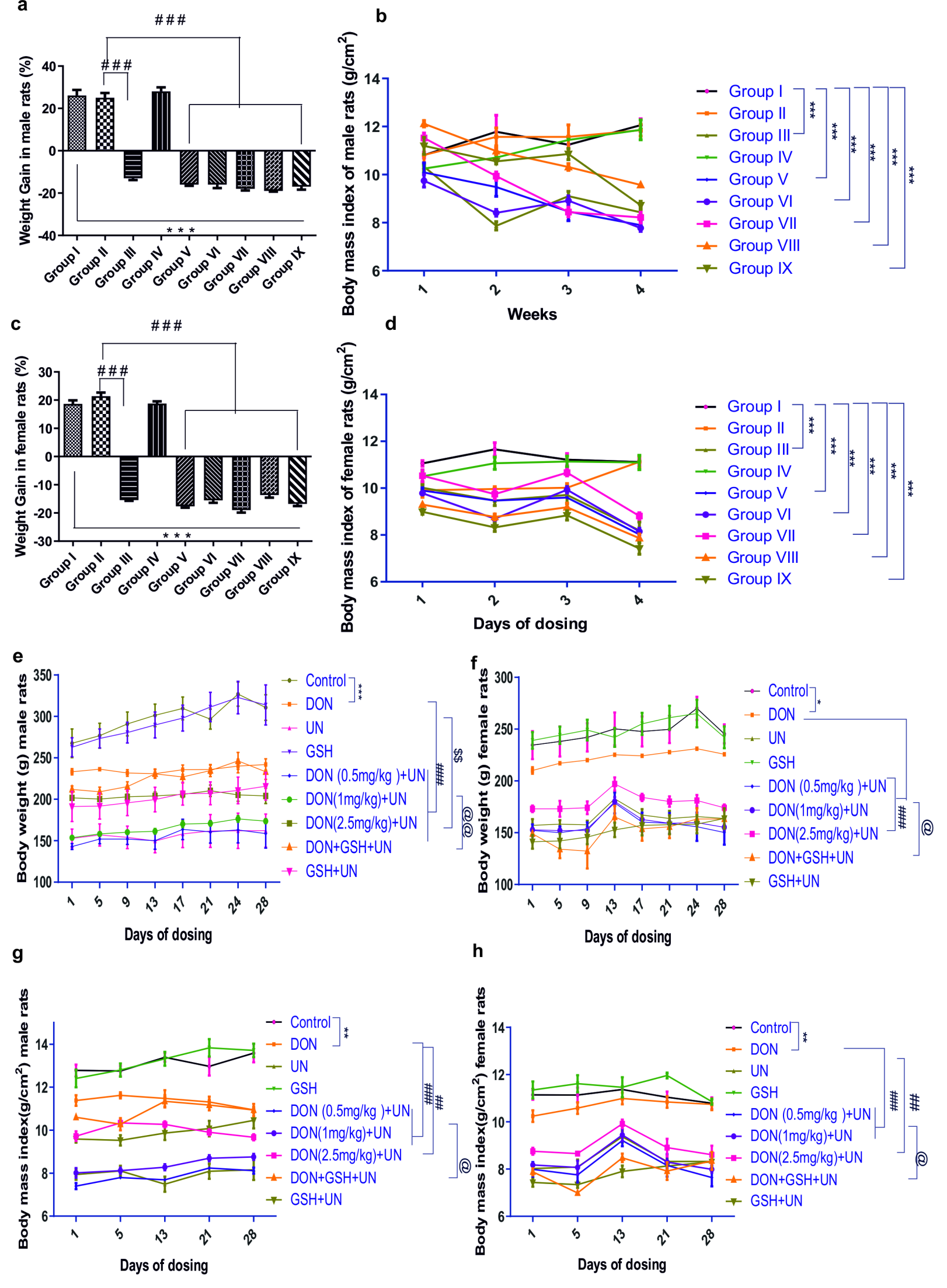
a
###
###
Weight Gain in male rats (%)
40
20
0
-20
-40
* * *
Group I
Group II
Group III
Group IV
Group V
Group VI
Group VII
Group VIII
Group IX
b
Body mass index of male rats (g/cm2)
14
12
10
8
6
1
2
3
4
Weeks
Group I
Group II
Group III
Group IV
Group V
Group VI
Group VII
Group VIII
Group IX
***
c
###
###
Weight Gain in female rats (%)
30
20
10
0
-10
-20
-30
* * *
Group I
Group II
Group III
Group IV
Group V
Group VI
Group VII
Group VIII
Group IX
d
Body mass index of female rats (g/cm2)
14
12
10
8
6
1
2
3
4
Days of dosing
Group I
Group II
Group III
Group IV
Group V
Group VI
Group VII
Group VIII
Group IX
***
e
Body weight (g) male rats
350
300
250
200
150
100
1
5
9
13
17
21
24
28
Days of dosing
Control
DON
UN
GSH
DON (0.5mg/kg)+UN
DON(1mg/kg)+UN
DON(2.5mg/kg)+UN
DON+GSH+UN
GSH+UN
***
###
$$
@@
f
Body weight (g) female rats
300
250
200
150
100
1
5
9
13
17
21
24
28
Days of dosing
Control
DON
UN
GSH
DON (0.5mg/kg)+UN
DON(1mg/kg)+UN
DON(2.5mg/kg)+UN
DON+GSH+UN
GSH+UN
*
###
@
g
Body mass index(g/cm2) male rats
14
12
10
8
6
1
5
13
21
28
Days of dosing
Control
DON
UN
GSH
DON (0.5mg/kg)+UN
DON(1mg/kg)+UN
DON(2.5mg/kg)+UN
DON+GSH+UN
GSH+UN
**
###
##
@
h
Body mass index(g/cm2) female rats
14
12
10
8
6
1
5
13
21
28
Days of dosing
Control
DON
UN
GSH
DON (0.5mg/kg)+UN
DON(1mg/kg)+UN
DON(2.5mg/kg)+UN
DON+GSH+UN
GSH+UN
**
###
##
@

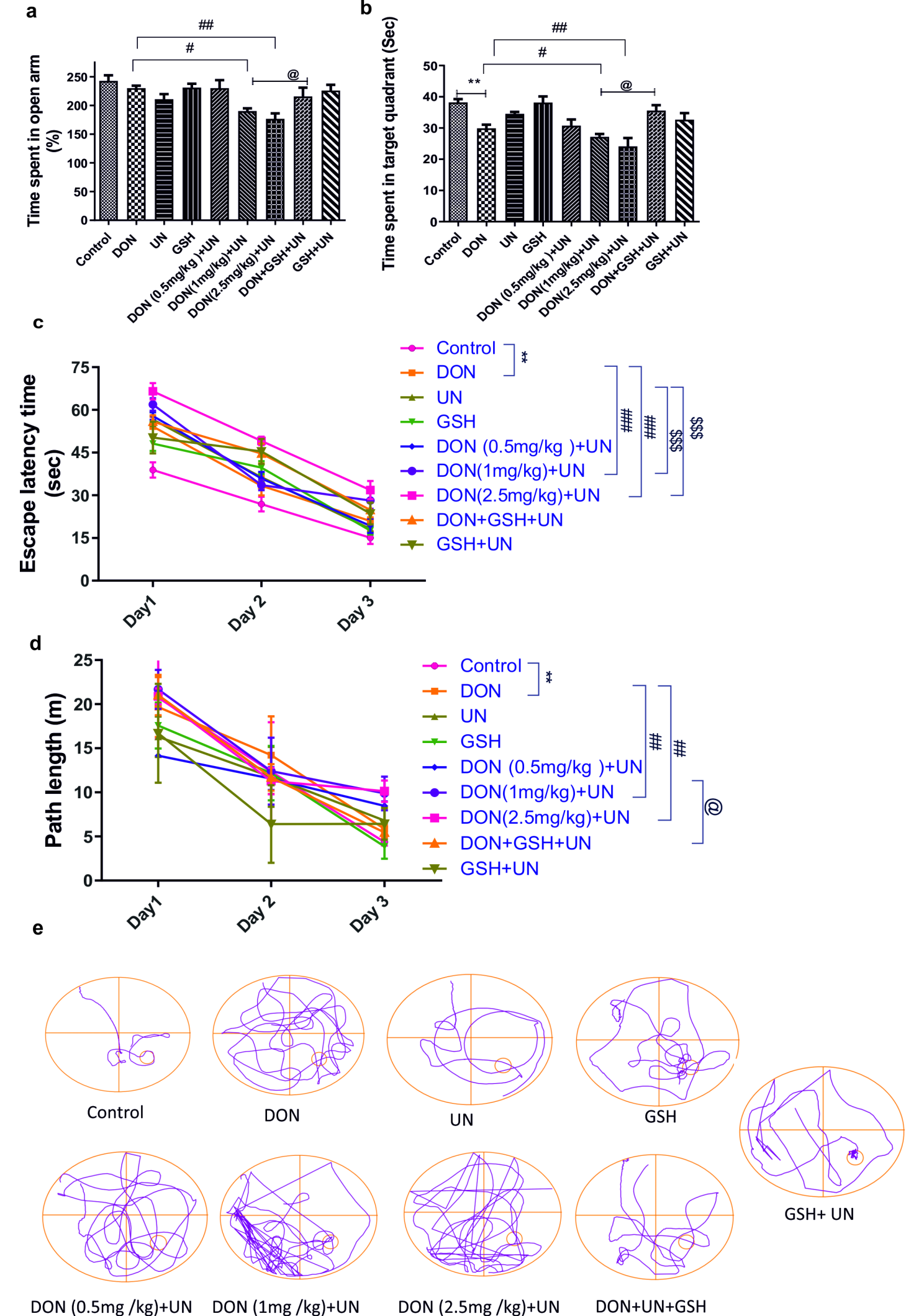
a
Time spent in open arm (%)
##
#
@
Control
DON
UN
GSH
DON (0.5mg/kg)+UN
DON(1mg/kg)+UN
DON(2.5mg/kg)+UN
DON+GSH+UN
GSH+UN
b
Time spent in target quadrant (Sec)
**
c
Escape latency time (sec)
Day1
Day 2
Day 3
*
###
$$$
d
Path length (m)
**
##
@
e
Control
DON
UN
GSH
GSH+ UN
DON (0.5mg /kg)+UN
DON (1mg /kg)+UN
DON (2.5mg /kg)+UN
DON+UN+GSH

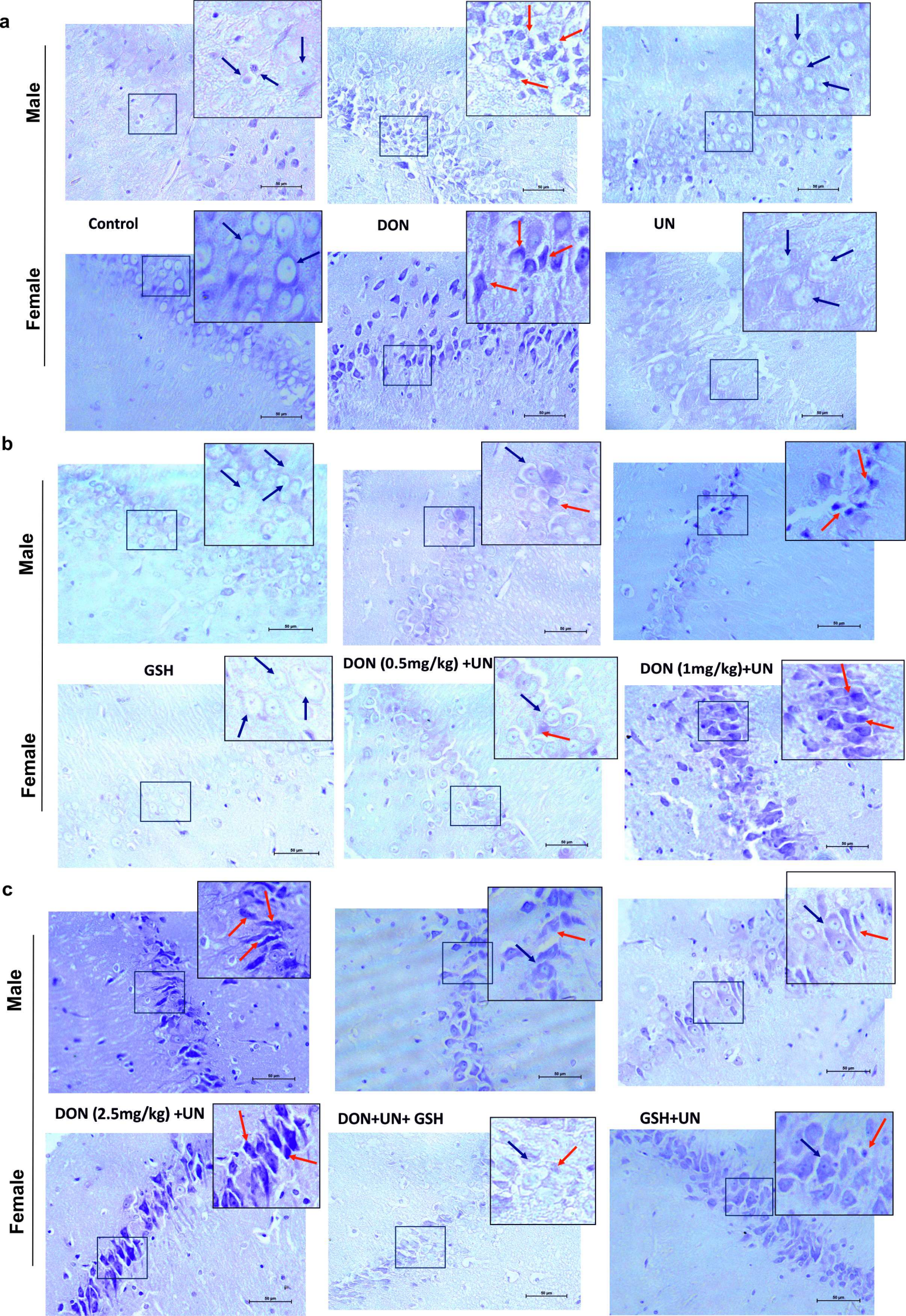
a
Male
Female
Control
DON
UN
b
Male
Female
GSH
DON (0.5mg/kg) +UN
DON (1mg/kg)+UN
c
Male
Female
DON (2.5mg/kg) +UN
DON+UN+ GSH
GSH+UN

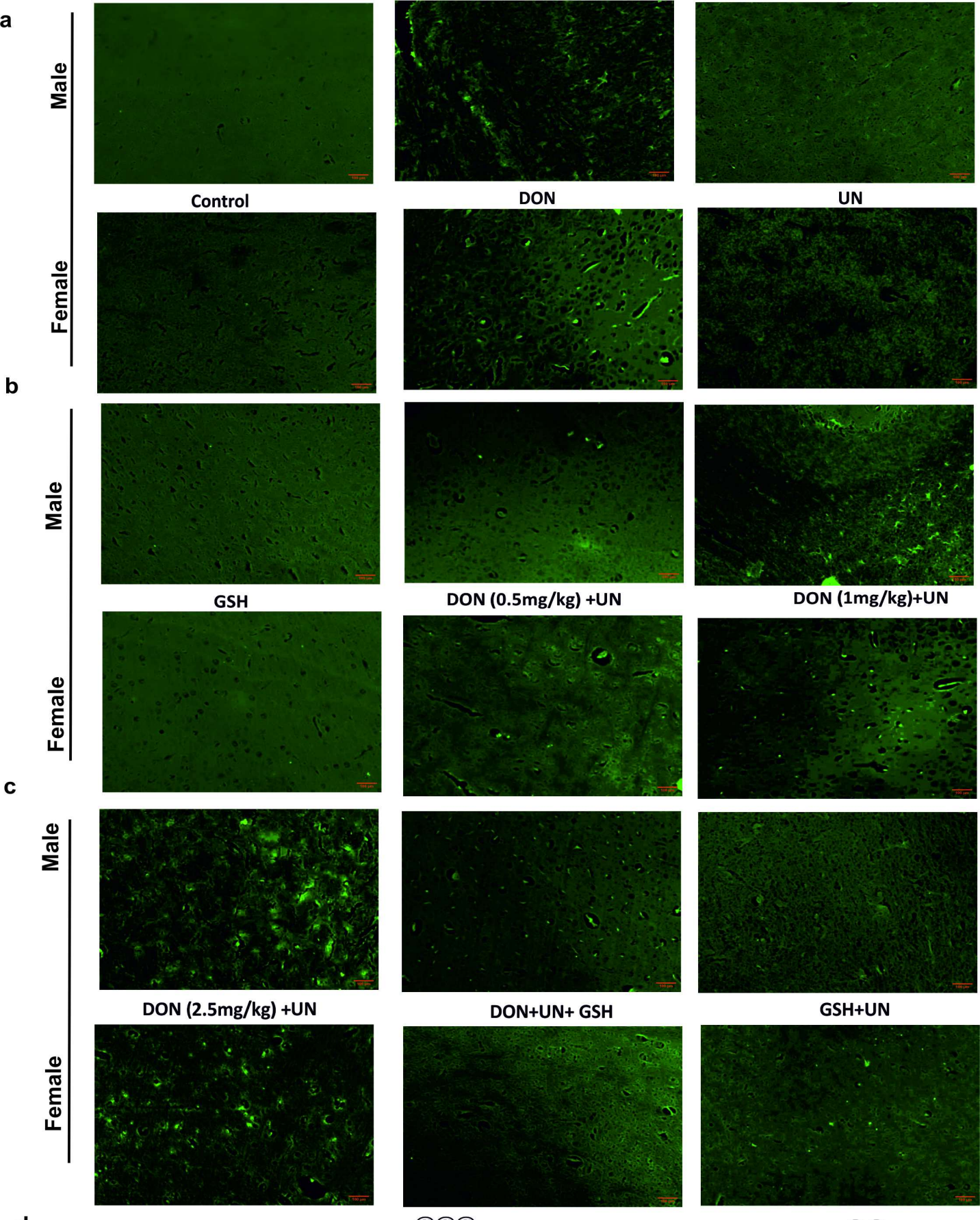
a
Male
Female
Control
DON
UN
b
GSH
DON (0.5mg/kg) +UN
DON (1mg/kg)+UN
c
DON (2.5mg/kg) +UN
DON+UN+ GSH
GSH+UN

d

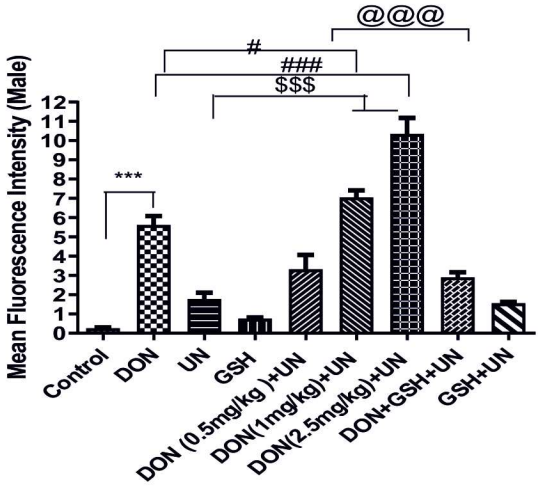
Mean Fluorescence Intensity (Male)
@@@
#
###
$$$
***
Control
DON
UN
GSH
DON (0.5mg/kg)+UN
DON(1mg/kg)+UN
DON(2.5mg/kg)+UN
DON+GSH+UN
GSH+UN

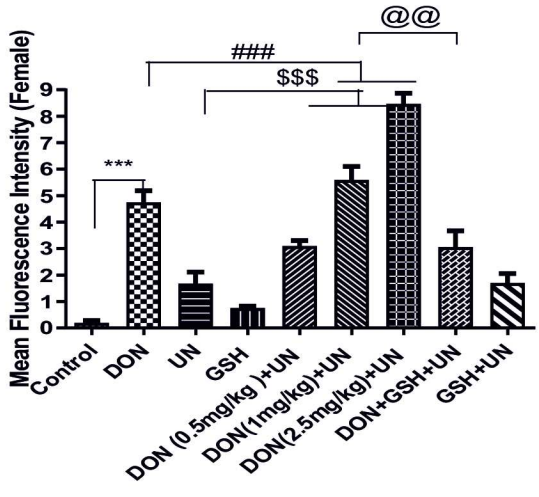
Mean Fluorescence Intensity (Female)
@@
###
$$$
***
Control
DON
UN
GSH
DON (0.5mg/kg)+UN
DON(1mg/kg)+UN
DON(2.5mg/kg)+UN
DON+GSH+UN
GSH+UN

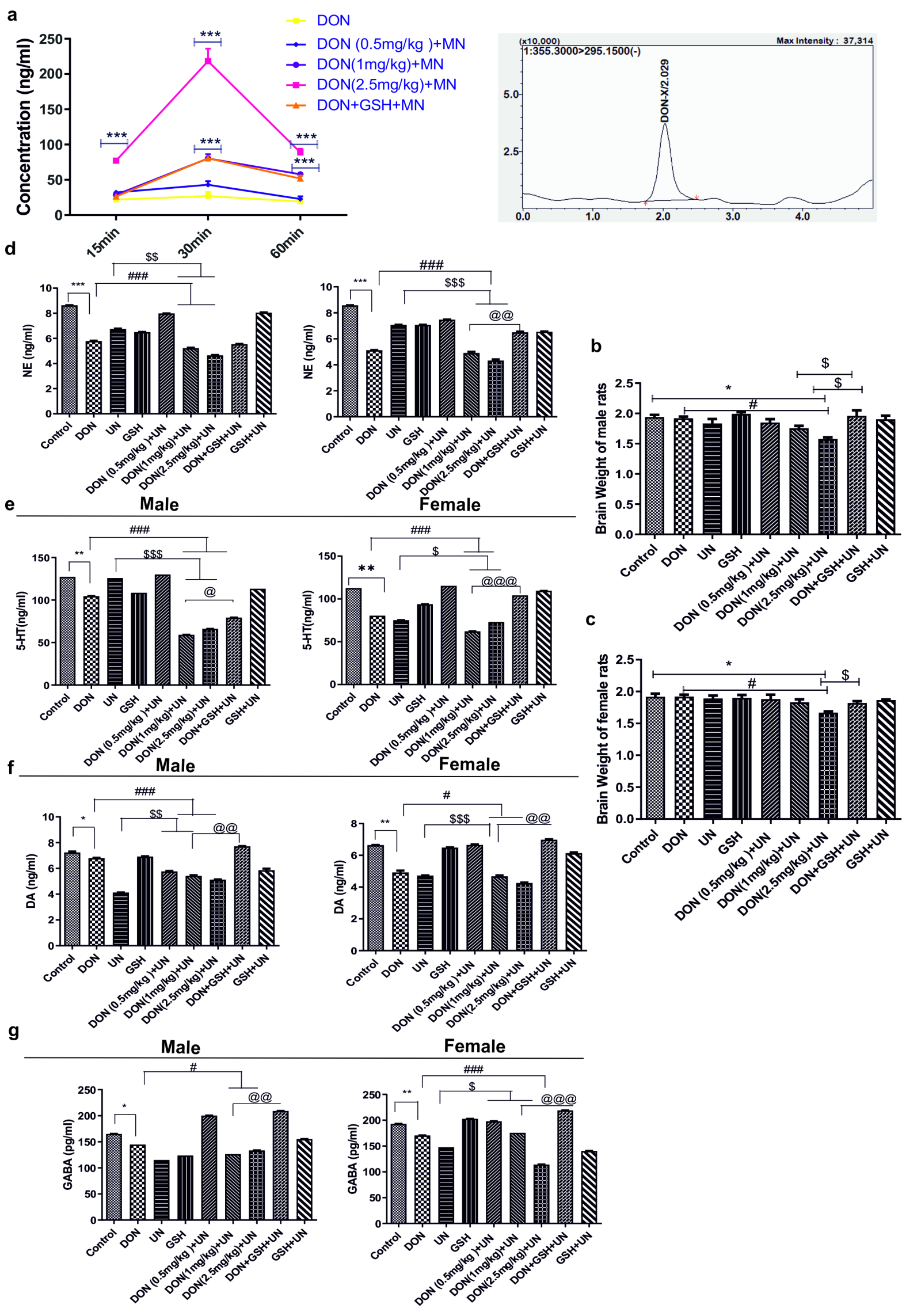
a
DON
DON (0.5mg/kg)+MN
DON(1mg/kg)+MN
DON(2.5mg/kg)+MN
DON+GSH+MN
Concentration (ng/ml)
15min
30min
60min
(x10,000)
1:355.3000>295.1500(-)
Max Intensity : 37,314
DON-X/2.029
b
Brain Weight of male rats
c
Brain Weight of female rats
d
NE (ng/ml)
Male
Female
e
5-HT(ng/ml)
f
DA (ng/ml)
g
GABA (pg/ml)
Control
DON
UN
GSH
DON (0.5mg/kg)+UN
DON(1mg/kg)+UN
DON(2.5mg/kg)+UN
DON+GSH+UN
GSH+UN

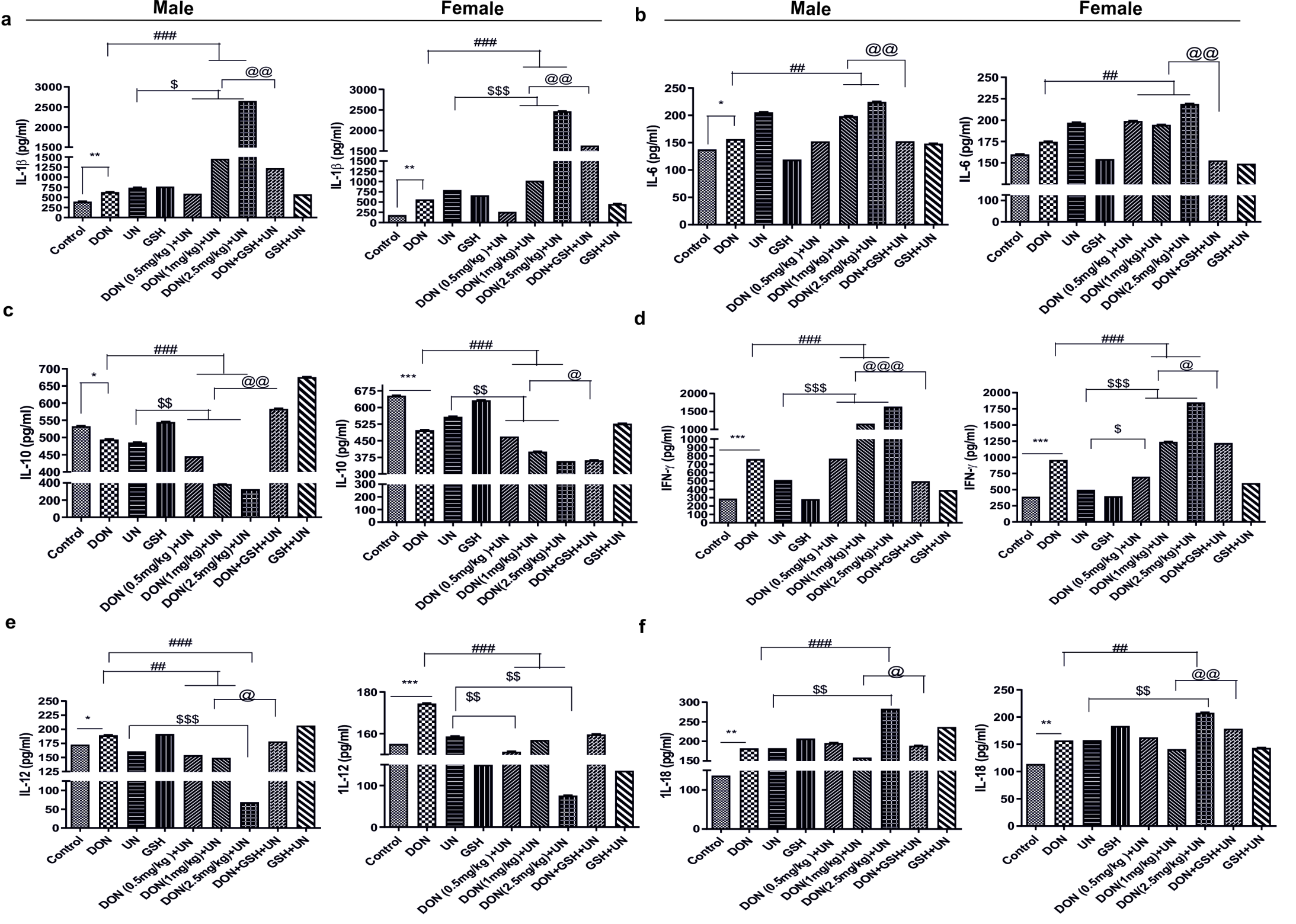
a
Male
Female
IL-1β (pg/ml)
b
IL-6 (pg/ml)
c
IL-10 (pg/ml)
d
IFN-γ (pg/ml)
e
IL-12 (pg/ml)
1L-12 (pg/ml)
f
1L-18 (pg/ml)
IL-18 (pg/ml)
Control
DON
UN
GSH
DON (0.5mg/kg)+UN
DON(1mg/kg)+UN
DON(2.5mg/kg)+UN
DON+GSH+UN
GSH+UN

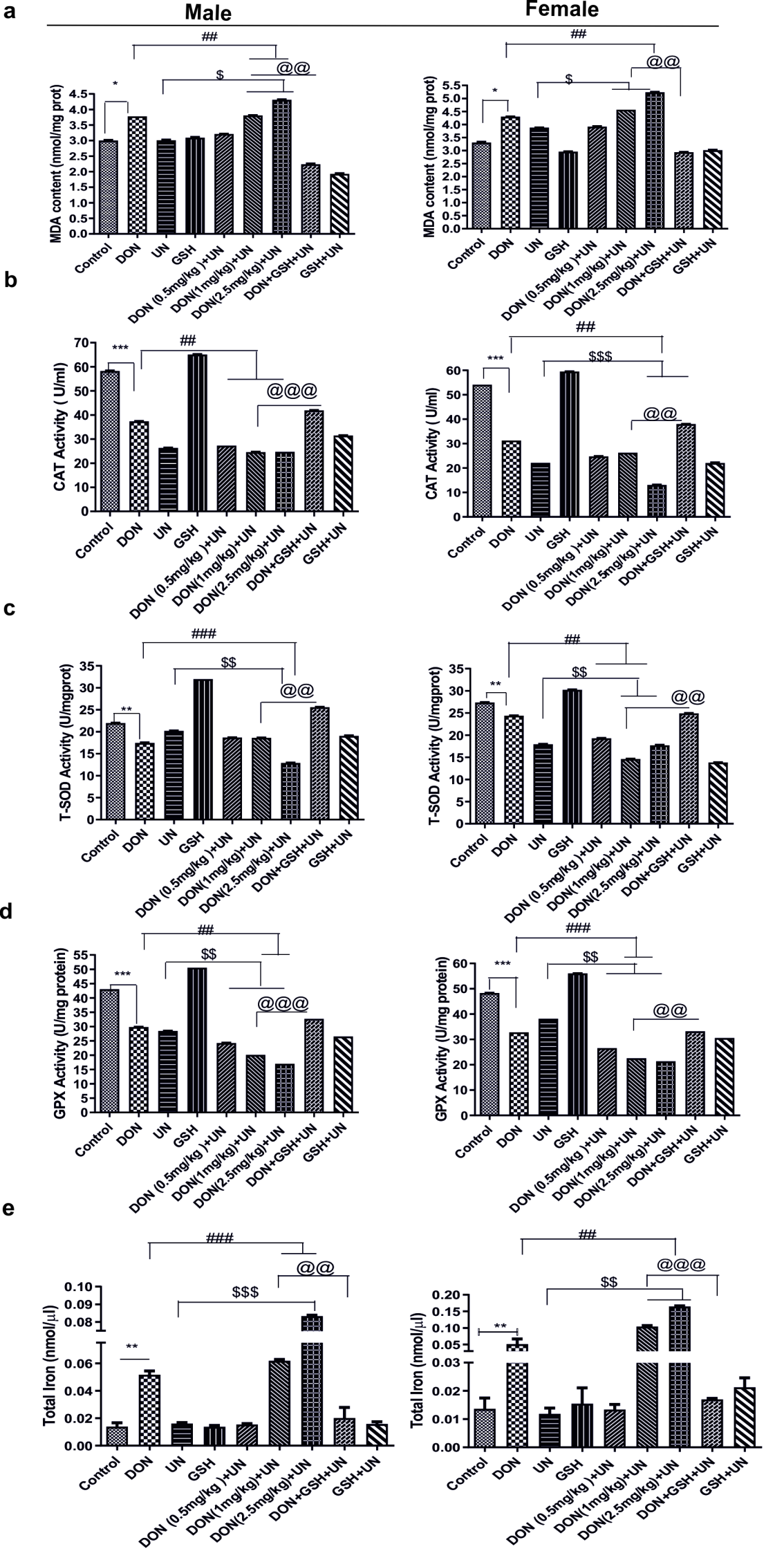
a
Male
Female
MDA content (nmol/mg prot)
b
CAT Activity (U/ml)
c
T-SOD Activity (U/mgprot)
d
GPX Activity (U/mg protein)
e
Total Iron (nmol/μl)
Control
DON
UN
GSH
DON (0.5mg/kg)+UN
DON(1mg/kg)+UN
DON(2.5mg/kg)+UN
DON+GSH+UN
GSH+UN

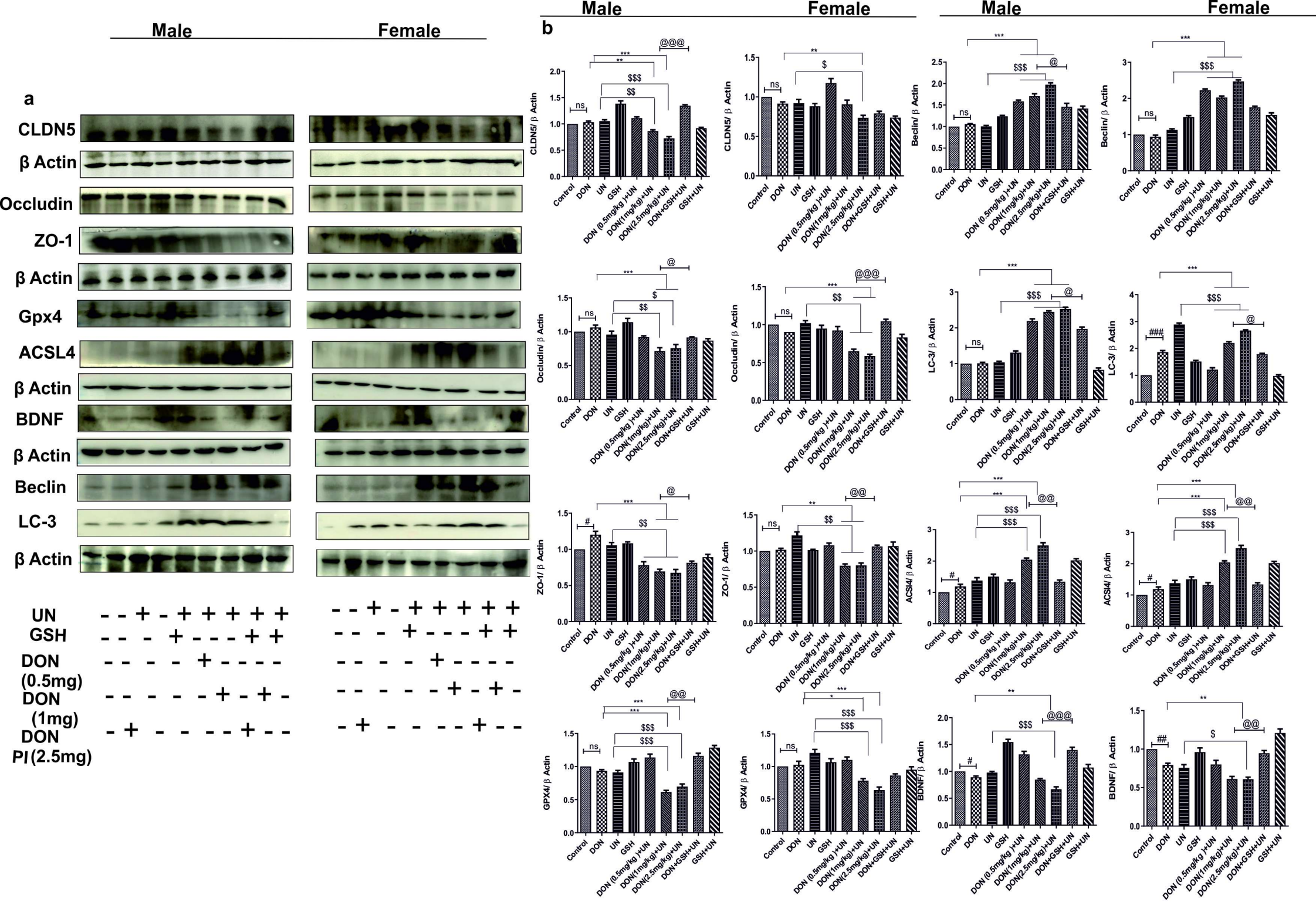
Male
Female
a
CLDN5
β Actin
Occludin
ZO-1
β Actin
Gpx4
ACSL4
β Actin
BDNF
β Actin
Beclin
LC-3
β Actin
UN
GSH
DON (0.5mg)
DON (1mg)
DON PI (2.5mg)
b
CLDN5/ β Actin
Beclin/ β Actin
Occludin/ β Actin
LC-3/ β Actin
ZO-1/ β Actin
ACSl4/ β Actin
GPX4/ β Actin
BDNF/ β Actin
Control
DON
UN
GSH
DON (0.5mg/kg)+UN
DON(1mg/kg)+UN
DON(2.5mg/kg)+UN
DON+GSH+UN
GSH+UN

Table 1. The table shows the optimized MS parameters of analyte, IS and instrument.

Ion-source parameters		**Values**
Interface temperature		300 ºC
Heat block temperature		400 ºC
Nebulizer gas		Nitrogen
Heating and drying gas		Nitrogen
Collision gas (CAD)		270 kPa
Voltage		5000 eV
Dwell time		100 msec
Polarity		Negative
Desolvation line temperature		250 ºC
Quadrupole resolution		1
Analyte parameters	**Compound DON**	**RSV(IS)**
Q1/Q3, *m/z*	355.3/295.15	480.2/418.15
Q1 Prebias	22	30
CE	10	15
Q3 Prebias	13	30

Q1- Precursor ion; Q3- Product ion; CE- Collision energy.

Table 2. Weight for age relationship (WA) Value for male and female rats

WA Values (Male)						
	DAY 1	**DAY 6**	**DAY 11**	**DAY 16**	**DAY 21**	**DAY 28**
Control	100%	100%	100%	100%	100%	100%
DON	94.90%	91.35%	106.05%	99.39%	100.45%	93.95%
UN	94.48%	62.75%	73.14%	74.32%	68.57%	64.32%
GSH	93.10%	85.05%	101.14%	97.85%	102.43%	99.60%
DON (0.5mg/kg)+UN	91.72%	75.41%	71.46%	67.88%	66.17%	67.85%
DON(1mg/kg)+UN	89.89%	67.59%	69.63%	73.03%	67.01%	66.22%
DON(2.5mg/kg)+UN	111.27%	86.51%	90.51%	74.61%	74.35%	67.52%
DON+GSH+UN	119.63%	92.92%	96.45%	87.93%	80.84%	63.77%
GSH+UN	106.89%	87.83%	90.28%	92.69%	83.80%	68.97%

WA Values (Female)						
	DAY 1	**DAY 6**	**DAY 11**	**DAY 16**	**DAY 21**	**DAY 28**
Control	100%	100%	100%	100%	100%	100%
DON	87.68%	89.07%	88.14%	89.13%	89.37%	94.43%
UN	88.24%	82.86%	81.88%	81.49%	74.26%	66.31%
GSH	95.98%	101.48%	102.22%	101.21%	101.57%	101.35%
DON (0.5mg/kg)+UN	89.78%	83.48%	71.55%	80.61%	70.09%	65.94%
DON(1mg/kg)+UN	86.87%	75.41%	70.96%	81.64%	71.09%	65.20%
DON(2.5mg/kg)+UN	96.38%	88.76%	81.77%	81.93%	77.00%	69.36%
DON+GSH+UN	83.33%	76.50%	76.74%	76.06%	69.37%	63.91%
GSH+UN	81.84%	73.44%	67.88%	73.67%	65.30%	60.61%

Supplementary Files

This is a list of supplementary files associated with this preprint. Click to download.

- S1.docx